Selenology Today

Lunar Domes

Properties and Formation Processes

Raffaello Lena
Christian Wöhler
James Phillips
Maria Teresa Chiocchetta

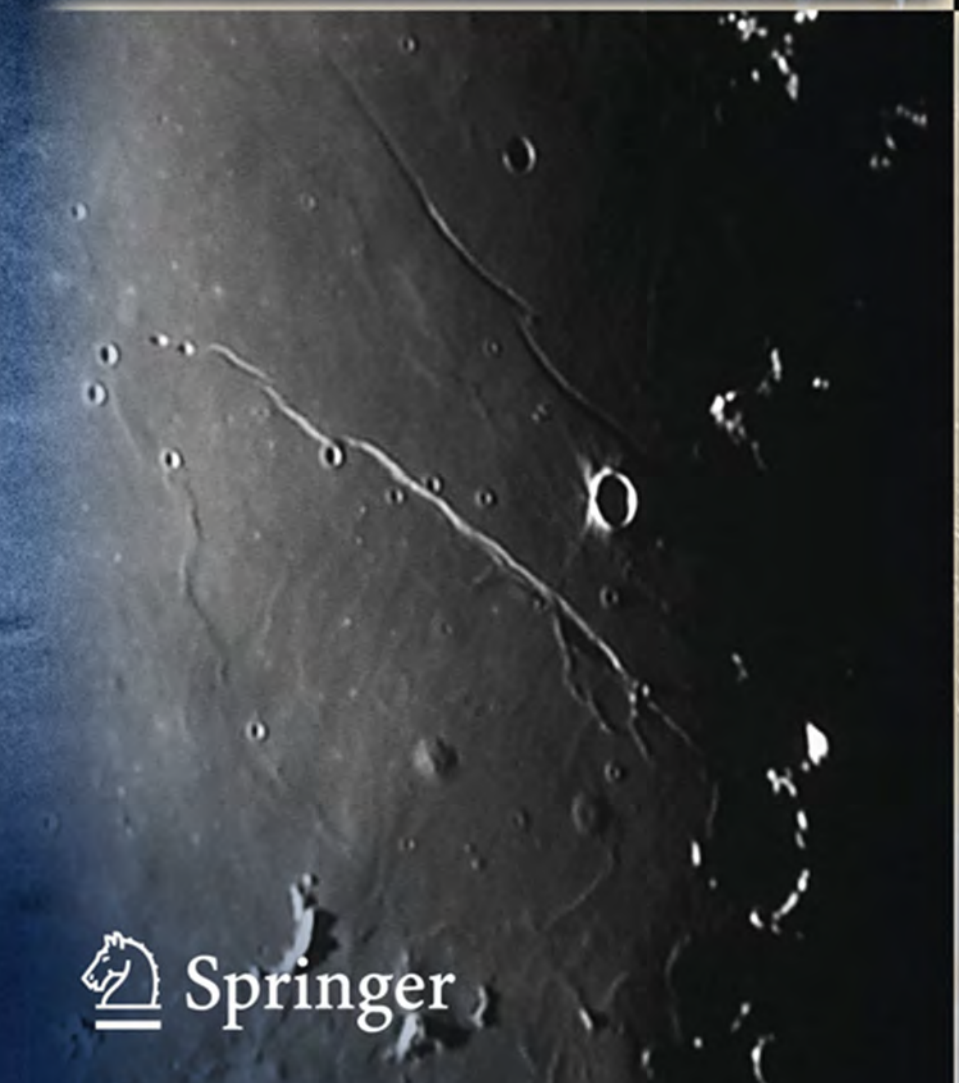

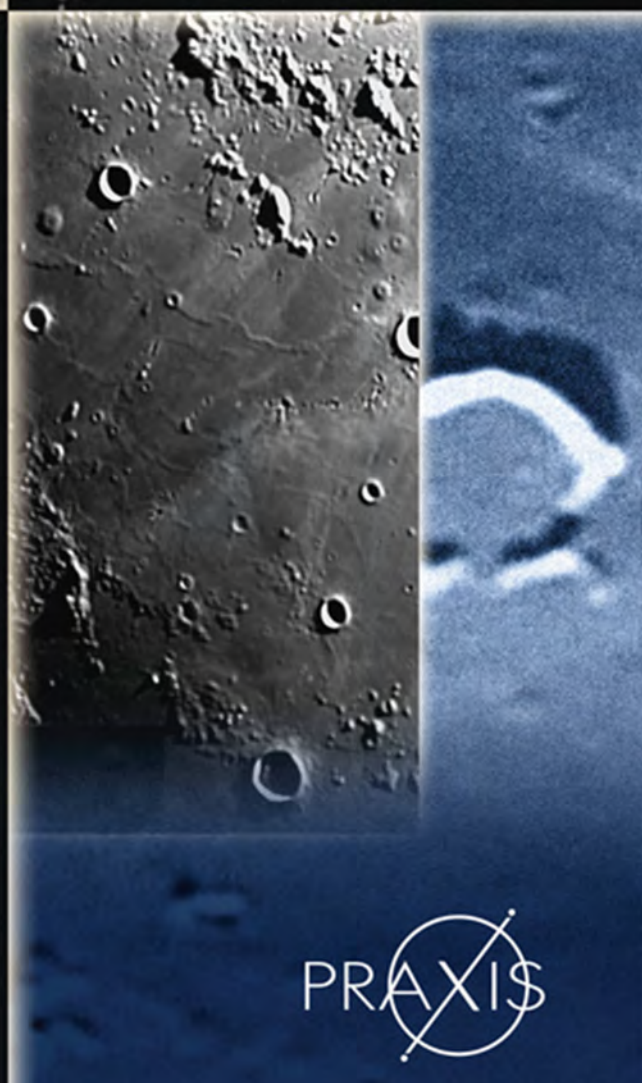

Springer

PRAXIS

ISSUE # 32, 2013

Selenology Today

Selenology Today is devoted to the publication of contributions in the field of lunar studies. Manuscripts reporting the results of new research concerning the astronomy, geology, physics, chemistry and other scientific aspects of Earth's Moon are welcome. Selenology Today publishes papers devoted exclusively to the Moon. Reviews, historical papers and manuscripts describing observing or spacecraft instrumentation are considered.

Selenology Today website
http://digilander.libero.it/glrgroup/

and here you can found all older issues
http://www.lunar-captures.com/SelenologyToday.html

In this issue of Selenology Today not only Moon
(see the contents in following page).

Selenology Today is under a reorganization, so that further comments sent to us will help for the new structure. So please doesn't exit to contact us for any ideas and suggestion about the Journal. Comments and suggestions can be sent to Raffaello Lena editor in chief : gibbidomine@libero.it

ISSUE # 32, 2013

Selenology Today

Contents

COVER

Lunar Domes

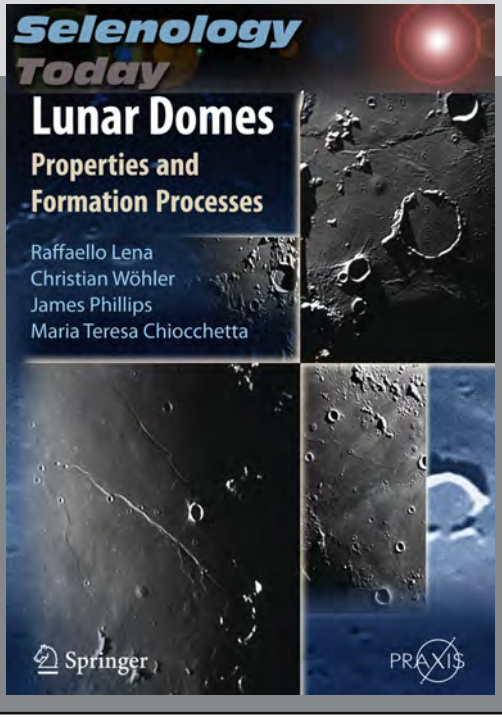

ISSUE # 32, 2013

Selenology Today

Observations on the uprange ejecta of oblique angle impact craters

Barry Fitz-Gerald GLR Group

Abstract

Oblique impacts are known to produce a suite of features within the ejecta blanket and on the planforms of the resulting craters. These changes only become evident at shallow impact angles, with initially the ejecta becoming sparse uprange, and then with the progressive appearance of a Zone of Avoidance (ZoA) or Forbidden Zone in the uprange direction, where ejecta appears to be poorly developed or absent. The crater planform remains circular at these impact angles and only departs from the axisymmetric at extremely low angles. The edges of theses ZoA's are in many cases defined by conspicuous rays which can, in some cases have a positive relief core, which survives as a topographic feature long after the bright ray material has become inconspicuous due to space weathering. The current article discusses this process, and relates it to features observed in the uprange ejecta blankets of a number of craters of proposed low angle origin. These features form uprange ridges which appear to form in the transition regime between craters that form ZoA,s and craters that exhibit more asymmetric ejecta such as the well known 'butterfly' pattern of crossrange rays.

The effects of low angle crater forming impacts has been discussed extensively, explored empirically and observed on the surfaces of the terrestrial planets (Gault & Wedekind,1978 and Herrick & Forsberg-Taylor, 2003). Low angle impacts can have spectacular consequences on the planform of the resulting craters, with elongate forms such as Schiller and Messier being the most familiar examples. Experimental work indicates however that all but the shallowest impacts (<10°) produce essentially axisymmetric craters (Gault & Wedekind,1978) with the asymmetry introduced by the impact angle only being evident in the distribution of the ejecta. This and later work demonstrated that in oblique impacts the ejecta curtain is initially tilted downrange but becomes more 'upright' as the cratering flow field undergoes the transition from that of a moving point source to that of a stationary point source later in the cratering process (Schultz, et.al, 2000 and Elbeshausen & Wünnemann 2013). This phenomenon will have an effect on the uprange and downrange ejecta, with one aspect being the development of the uprange Zone of Avoidance. Spectacular ZoA's are seen in the uprange ejecta of Proclus, Petavius B, Jackson, Ohm and Crookes. In these craters the ZoA's are defined laterally by bright cardioid (curving or heart shaped) or arachnid (straighter) rays. These bright rays will however, over time, become less prominent as radiation darkening and space weathering reduces the contrast between the rays and the surface on which they lie. As the associated craters will be approximately axisymmetric, evidence for the oblique nature of the impact will therefore disappear. In a number of cases however evidence of the ZoA is preserved in the form of a pair of diverging ridges, which originally formed the rays bounding the ZoA.

Cauchy and Kies A are probable examples of this category of oblique impact, with the diverging ridges forming 'wing' like extensions in the uprange directions (Wood 2011 & 2012). The 'wings' of Cauchy are composed of a combination of positive relief ridges proximally, which grade distally into elongate secondary craters and short intervening ridges arranged in an en-echelon configuration (Fig.1). This would appear to reflect the transition from the initial high angle, high velocity ejecta distally, to the lower angle lower velocity ejecta proximally. In the case of Kies A the distal crater chain sections are obscure whilst the proximal ridges are highly conspicuous particularly under low angle illumination (Fig.2).

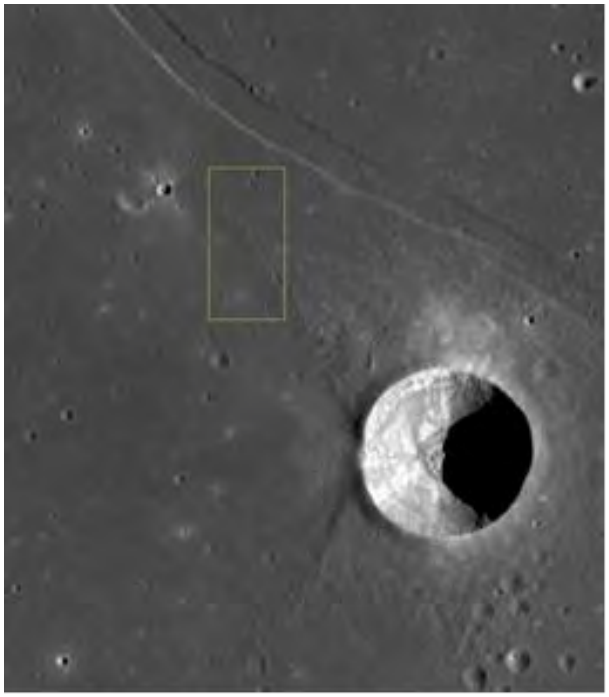

a.

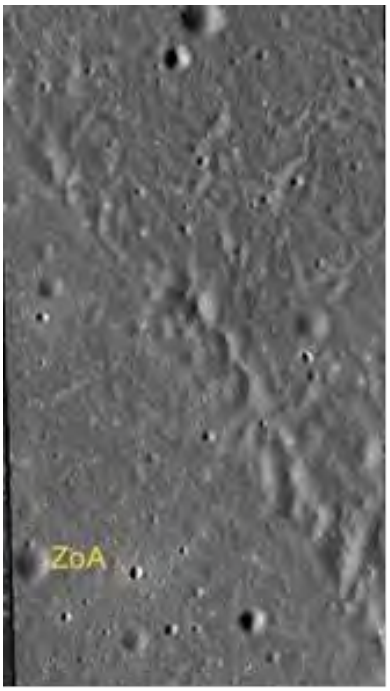

b.

Fig.1 Cauchy as seen by SELENE in this morning view (a) showing 'wings' to the north-west and south-west, and LROC NAC image of yellow box showing the en-echelon secondary craters and ridges which form the distal section of the wing (b). Note sparsity of ejecta within ZoA as compared to that north of the 'wing' .

Fig.2 LROC WAC image of Kies A showing positive relief proximal sections of 'wings' to the west. Note the cleft in the crater shadow as sun shines through the low point on the craters uprange rim.

A number of other craters exhibit similar structures but with the relative development of the ridge and crater chain elements in the 'wings' varying. One example is the 10km diameter Democritus A, which possesses a pair of long filamentous features which can be traced for over 30kms to the east and south-west (Fig.3). The distal section of these 'wings' appear to be composed of bifurcating linear grooves formed by complex arrangements of 'en echelon' secondary craters as noted above.

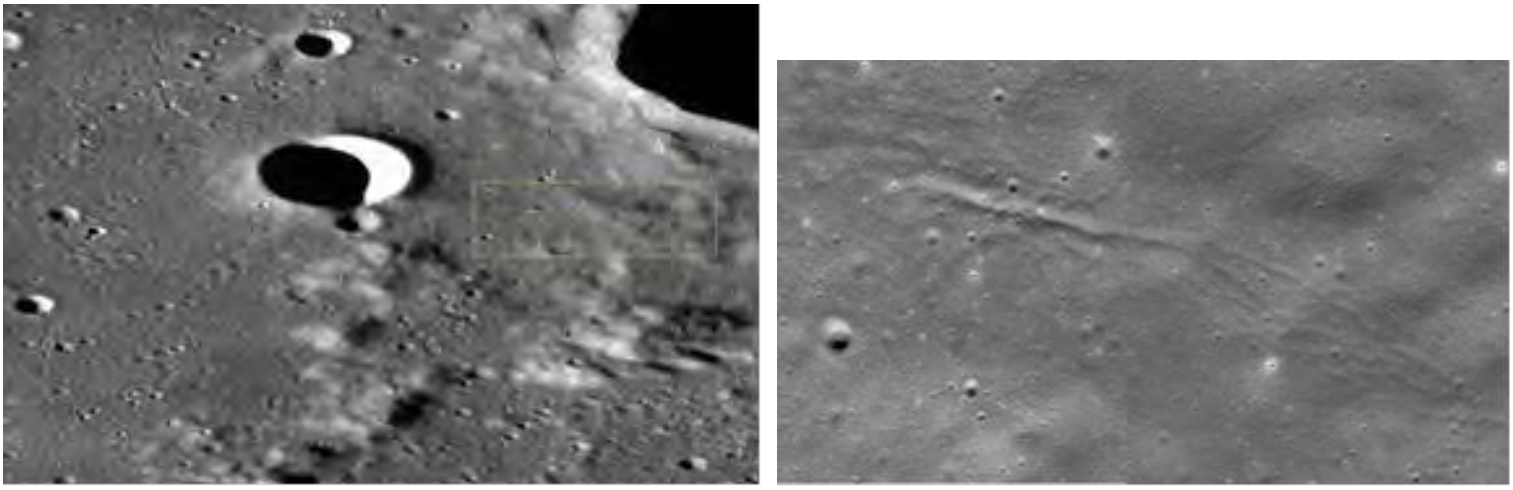

a. b.

Fig.3 LROC Quickmap image of Democritus A showing 'wings' to the east and south-west (a) and LROC NAC detail of area shown in yellow box showing bifurcating groove morphology of this distal section.

Cauchy, Kies A and Democritus A show their low angle credentials in the form of their rim morphology, with the uprange rim being depressed relative to the downrange rim (Fig.4), a phenomenon considered characteristic of hypervelocity low angle impacts (Forsberg, et.al, 1998).

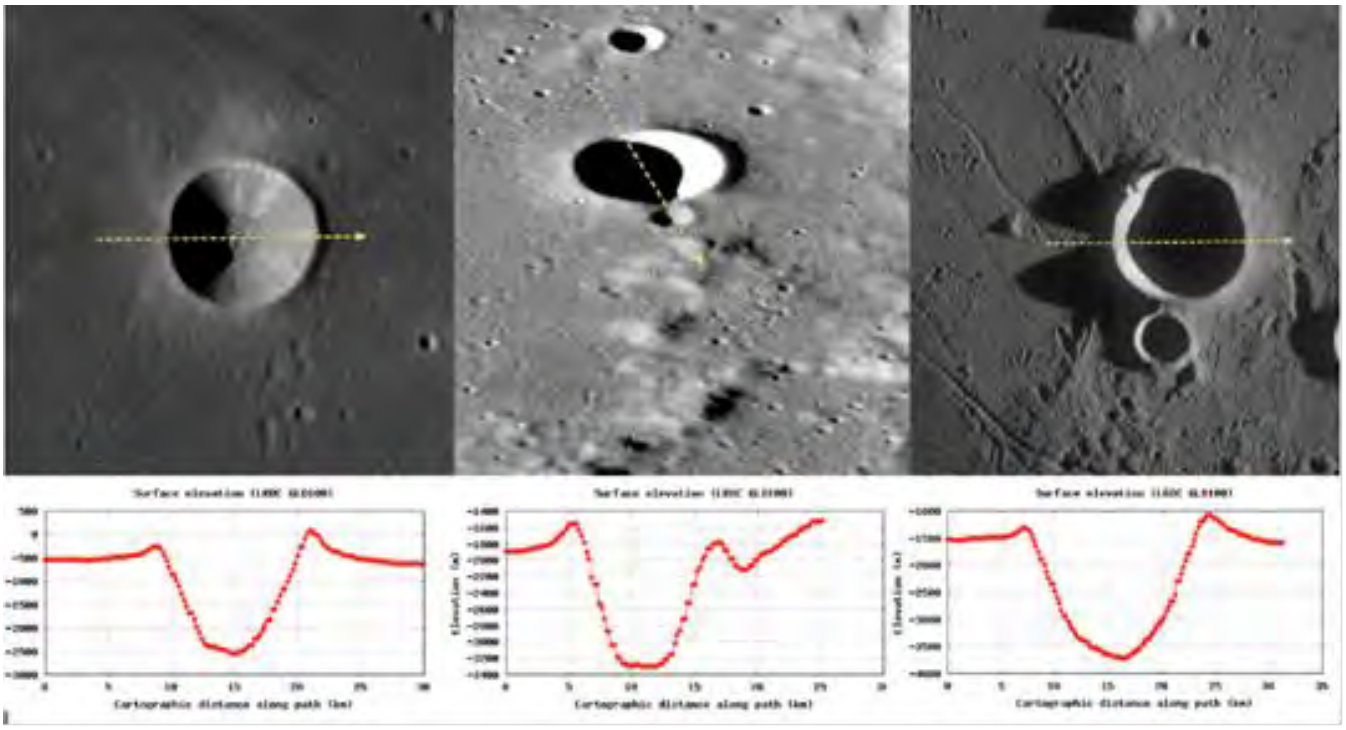

Fig.4 Surface elevation profiles as shown by LROC GLD100 for Cauchy, Democritus A and Kies A, showing depressed rim height uprange. Profiles taken along axis and direction shown by yellow arrows.

The example of Cauchy demonstrates that these wings appear to coincide with the edges of the ZoA, within which ejecta is sparse (Fig.1b). These ridges may form as the result of material excavated by secondary craters lining up in an en-echelon manner as seen in the distal sections of the wings in Cauchy (Fig.1) or as a result of deposition of material (possibly directly from the ejecta curtain) as demonstrated in the proximal sections of the wings of Kies A (Fig.2). It is possible that both processes occur in sequence during the crater forming process, with the formation of the proximal and distal parts of the 'wings' dominated by different processes. This might result in an initial secondary crater forming dominated phase giving rise to the distal sections and a depositional phase the proximal sections. This interpretation is supported by the observation that a similar configuration of proximal ridge and distal en-echelon crater chains can be seen to form the bright rays bordering the ZoA's of craters such as Proclus and Petavius B.

The uprange ejecta of the 12km diameter crater Markov E may possess another class of ridge like feature produced in oblique angle impacts. Markov E, whilst being more or less circular in outline has an asymmetric ejecta blanket where darker material has been excavated and deposited onto a lighter mare surface, whilst immediately proximal to the crater rim, bright deposits may represent the deepest excavated material of highland composition (Fig.5). The crater itself shows a depressed southern rim and a lack of ejecta in this direction, consistent with an impactor approaching from the south.

The lack of ejecta in the hypothesised uprange direction (south) is accompanied by the presence of an slightly sinuous ridge immediately uprange of the southern rim. This ridge is of very low relief (~ 50m high) and as noted above is slightly sinuous, giving an impression of short chevrons connected end to end.

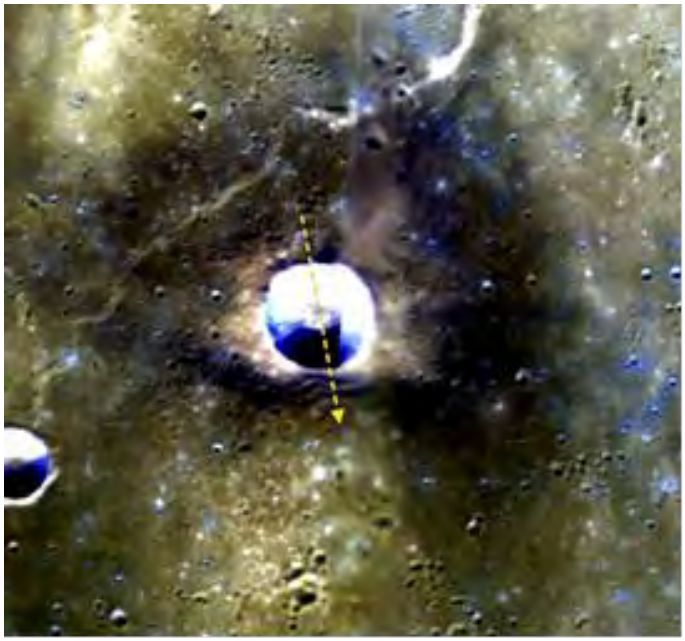

a.

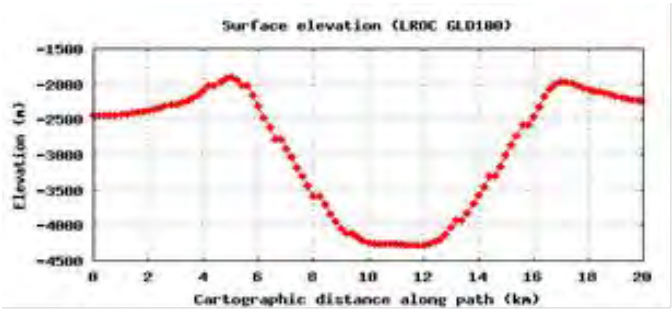

b.

Fig.5 Clementine UVVIS Multispectral Mosaic of Markov E showing asymmetric ejecta (a) and Surface elevation profiles as shown by LROC GLD100 (b). Profile taken along axis

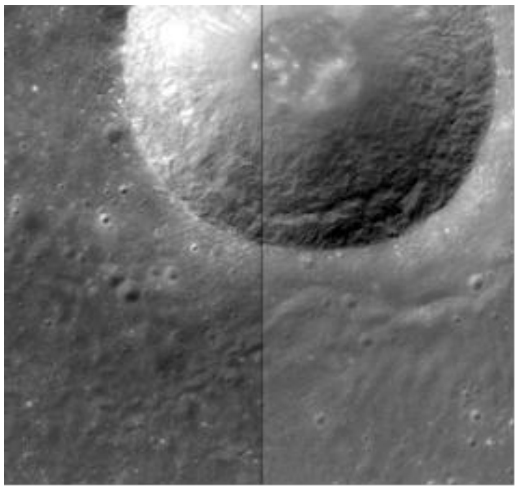

Fig.6 LROC NAC montage of uprange chevron ridge to the south of Markov E. Note the manner in which the ridge grades into the surrounding uprange ejecta, particularly the deceleration dunes to the west.

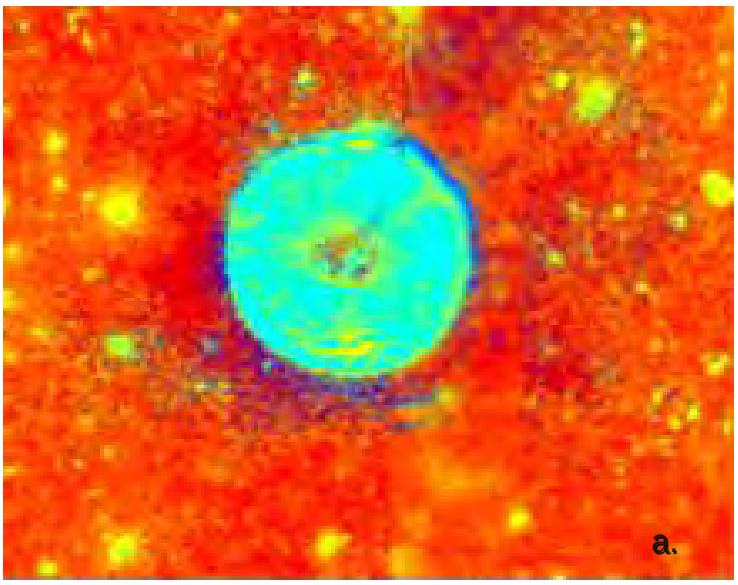

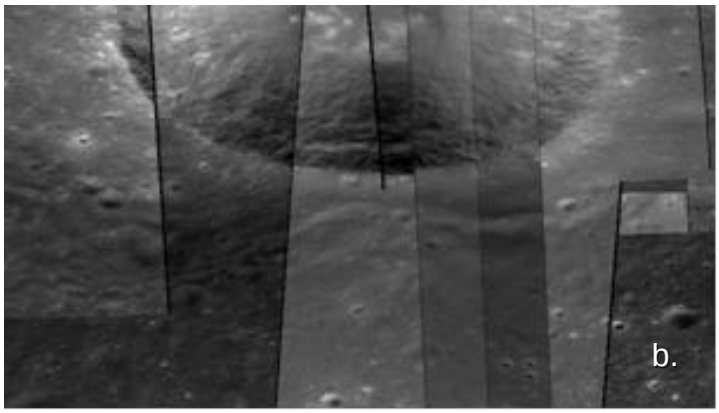

Fig.7 Clementine UV-VIS Ratio Map of Markov E showing compositional relationship between the chevron ridge and adjacent near rim ejecta (a) and LROC Quickmap image of ridge and dune field.

The ridge is approximately 10kms in length and is orientated roughly tangential to the southern rim of Markov E. That this ridge is part of the ejecta blanket and not a later tectonic feature (such as a wrinkle ridge) is indicated by the manner in which it grades into the surrounding ejecta, particularly a small field of imbricating deceleration dunes to the west, which also exhibit a subtle chevron configuration (Fig.6).

This relationship is further suggested by the Clementine UV-VIS Ratio Map image of Markov E that shows that the ridge and dune field share the same blue spectral signature of highland anorthosite also evident in the near rim ejecta (Fig.7a). This would indicate a similar origin during crater formation when deeply buried highland material was excavated and deposited immediately outside the rim. These observations indicate that this chevron ridge originated during crater excavation and represents a feature of the continuous ejecta blanket.

A similar ridge like feature may be seen within close proximity of the north-eastern rim of

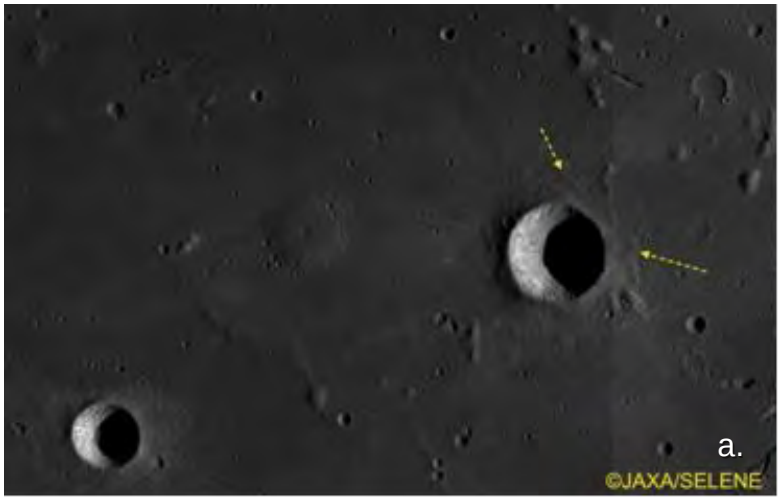

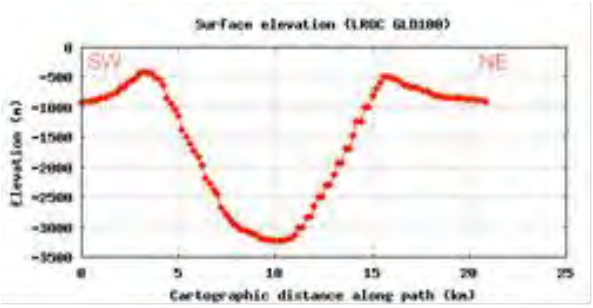

b.

Fig.8 Selene montage of Milichius showing possible ridge in uprange ejecta to the north-east (a) and Surface elevation profiles as shown by LROC GLD100 showing slightly depressed north-eastern rim (b). Note butterfly ejecta pattern in Milichius A (in

low elevation and approximately 1km wide, taking the form of gentle curve, tangential to the crater rim. Indications of oblique impact in the crater are however tenuous at best, with a very slightly depressed rim to the north-east, but the location of the ridge adjacent to the rim low point is suggestive (Fig.8).

The relationship of these tangential uprange ejecta features to oblique impacts is demonstrated in a couple of examples where the impacts occurred on inclined surfaces, which may in effect mimmic an oblique impact on a horizontal surface. One example, a bright youthful crater approximately 2kms in diameter, is located just inside the western rim of Galvani B, and appears to represent an impact on the slopes of the inner crater wall. The glancing nature of the impact appears to have resulted in an exceedingly shallow crater (Fig.9), in all probability heavily modified post impact by downslope movement of loose debris. In this case the impactor appears to have approached from the north-west and in this direction we see a field of tangentially arranged crater chains exhibiting an en-echelon chevron pattern draped over the western glacis of Galvani B (Fig.10).

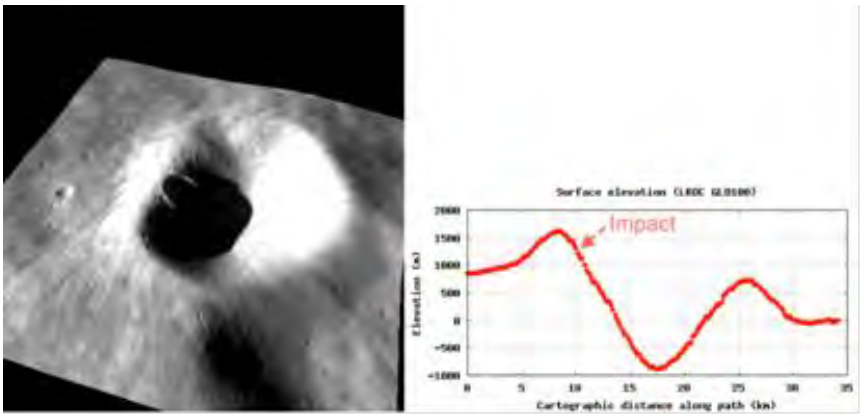

a.

Fig.9 LROC 3D Visualisation tool image of crater on western rim of Galvani B (a) and LROC GLD100 Surface elevation profiles showing position of impact (b).

concentrated crossrange but predominantly downrange as can be seen from the Clementine Ratio Map image (Fig.10c), with little ejecta in the uprange direction.

This might indicate that the impact angle was lower than that required to produce a ZoA and approaching that where crossrange 'butterfly' patterns begin to become apparent.

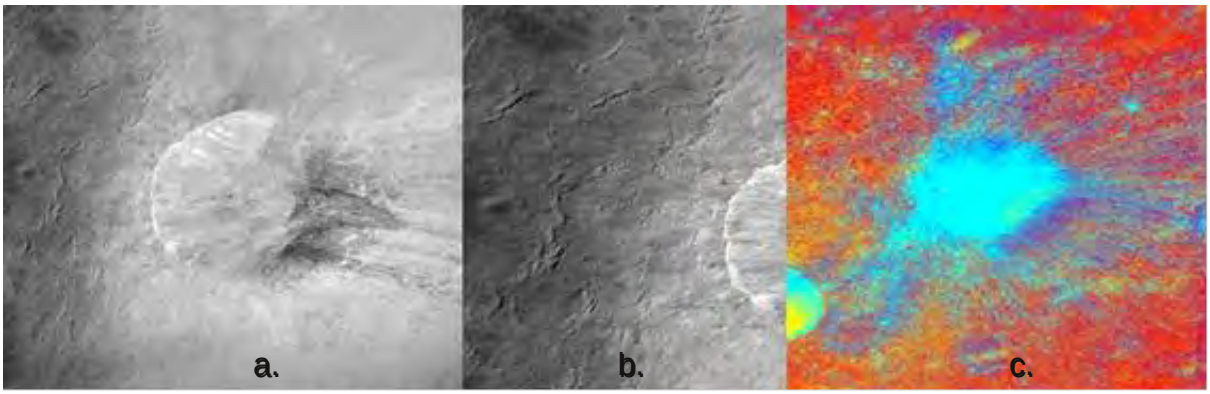

The asymmetry in the uprange and downrange ejecta configuration is striking, with the downrange (eastern) ejecta dominated by long rays without any suggestion of the tangential arrangement seen to the west. Bright ejecta is

Fig.10 LROC NAC montage (a) detail of uprange ejecta (b) and Clementine UV-VIS Ratio Map (b) of crater shown in Fig.9. Note lack of a ZoA.

The second example is another fresh 2km diameter crater located at the base of the north-western inner wall of Dante C. In this case the uprange direction corresponds to the north-western crater wall, and the downrange to the crater floor to the south-east. As with the previous example, a zone of tangentially arranged en-echelon crater chains exists uprange, which in this case 'wrap' slightly around the crater towards the downrange direction (Fig.11).

Both of these examples are clearly affected by the terrain on which they are developed, with slope playing a significant part in the final form of the ejecta and crater itself. They do however demonstrate the clear influence of impact angle on the ejecta pattern, especially on the production of these tangential uprange zones. Neither of the above has a ridge as observed in Markov E (or possibly Milichius) but it is possible to propose that as the impact angle decreases, this zone would become narrower in extent and eventually disappear at very low angles where uprange ejecta is altogether absent.

(12kms). Both craters have been discussed by Herrick & Forsberg-Taylor (2003) in relation to oblique lunar impact craters, with Dawes being described as having a rim asymmetry (ellipticity of < 1.1) and Sulpicius Gallus as being nearly axisymmetric despite being considered an oblique angle crater. Dawes has been the subject of considerable study with particular regard to its rim and floor topography. Rather less comment has been attracted by Rima Dawes, a linear trough type feature to the north-east. This feature is however not restricted to the north-east, but appears to wrap around the craters eastern rim, and is present to the south-east as a trough between two ridges. The trough is interrupted half way along its length by what appears to be an impact melt rich slump off the eastern rim, but the relationship between the northern and southern sections is clear and their mode of origin almost certainly related. This structure does not appear to be a pre-crater structure, and similarly is unlikely to be a product of post impact modification. Dawes itself shows clear indications

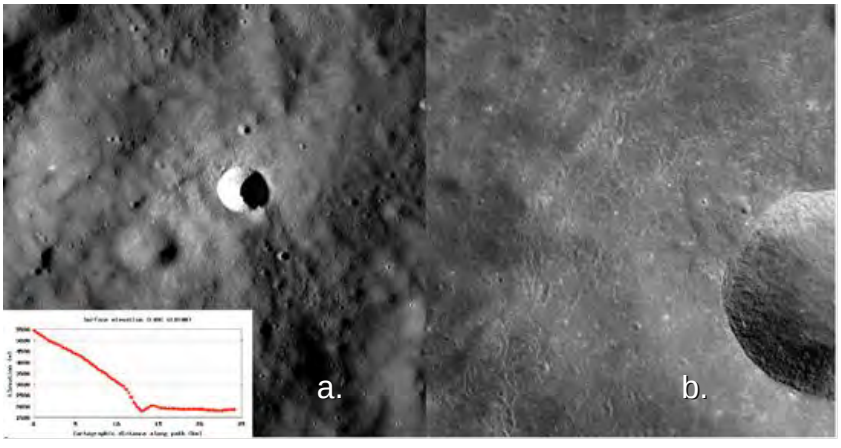

Fig.11 LROC Quickmap of crater on floor of Dante C, with GLD100 profile in inset to show position at base of inner crater wall (a) and detail of tangentially arranged ejecta uprange (b).

At some point therefore conditions might exist where the uprange ejecta becomes restricted to a very narrow zone, and is consequently concentrated into the type of ridge like feature we see in Markov E.

Further examples of the phenomenon proposed in the above discussion may be provided by the craters Dawes (17kms) and Sulpicius Gallus

of an oblique impact origin (Fig.12b) with the ejecta clearly divided into two components. One component is focussed downrange and is visible in this data as a yellow ray of presumably freshly fragmented mare material produced in the early phase of crater formation when the ejecta curtain was tilted downrange.

Further examples of the phenomenon proposed in the above discussion may be provided by the craters Dawes (17kms) and Sulpicius Gallus (12kms). Both craters have been discussed by Herrick & Forsberg-Taylor (2003) in relation to oblique lunar impact craters, with Dawes being described as having a rim asymmetry (ellipticity of < 1.1) and Sulpicius Gallus as being nearly axisymmetric despite being considered an oblique angle crater. Dawes has been the subject of considerable study with particular regard to its rim and floor topography. Rather less comment has been attracted by Rima Dawes, a linear trough type feature to the north-east. This feature is however not restricted to the north-east, but appears to wrap around the craters eastern rim, and is present to the south-east as a trough between two ridges. The trough is interrupted half way along its length by what appears to be an impact melt rich slump off the eastern rim, but the relationship between the northern and southern sections is clear and their mode of origin almost certainly related. This structure does not appear to be a pre-crater structure, and similarly is unlikely to be a product of post impact modification. Dawes itself shows clear indications of an oblique impact origin (Fig.12b) in the Clementine UVVIS data, with the ejecta clearly divided into two components. One component is focussed downrange and is visible in this data as a yellow ray of presumably freshly fragmented mare material produced in the early phase of crater formation when the ejecta curtain was tilted downrange.

Superimposed on this, and having a more symmetrical distribution is a deposit showing as light blue, and representing material excavated from deeper levels, but during a later phase in the process when the ejecta curtain had assumed a more 'upright' orientation. This shows that a symmetric and asymmetric ejecta pattern can be generated in the same impact event.The LROC GLD100 surface elevation plot also shows a slightly depressed eastern (uprange) rim, which is consistent with an impactor approaching from the east (Fig.12b).

Morphologically, Rima Dawes consists of adjacent, sub-parallel ridges either side of a depressed trough, and not a lunar surface feature such as a graben or sinuous rille (Fig.13). The inner ridge is narrower than the broad outer ridge,

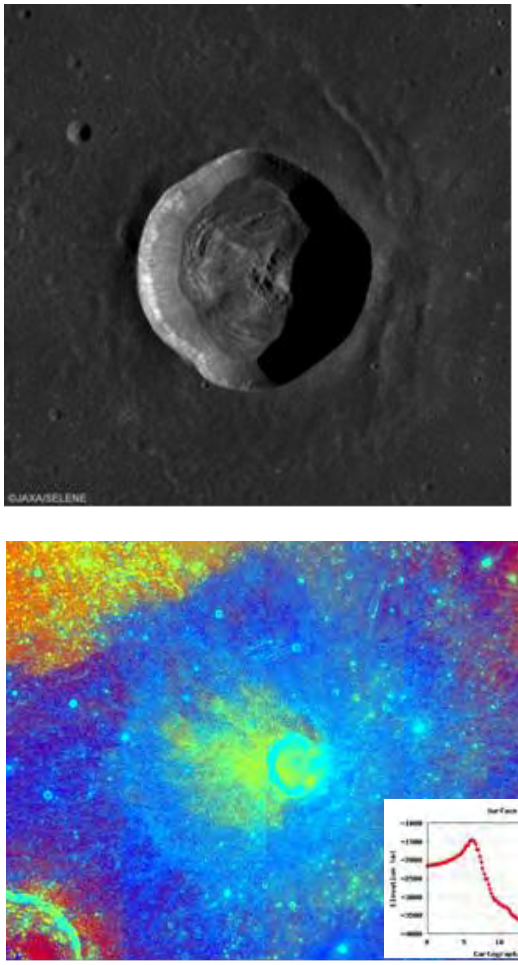

Fig.12 SELENE image of Dawes showing Rima Dawes to the north-east (a) and Clementine UVVIS Ratio Map and inset LROC GLD100 surface elevation plot showing evidence of oblique impact origin (b).

with an approximate elevation of a few tens of meters at the most for both features. Detailed views show that the ridges themselves have a veneer of impact melt, which is most apparent on the uprange aspect of the inner ridge where it can be seen to form a slightly 'stepped' texture, possibly where the edges of individual flow fronts have started to erode. The inner

ridge also has boulders perched its summit, strongly suggesting an origin during the impact process itself. The glacis between the inner ridge and the eastern rim also has a considerable covering of impact melt whilst immediately below the eastern rim considerable numbers of impact melt gullies can be seen. It is worth noting that the greatest development of impact melt appears to be in the north-east quadrant, somewhat at odds with the oblique impact from the east. This melt distribution may however have more to do with melt displacement during the complex wall slumping processes that occurred during the crater modification stage rather than processes occurring during the impact event itself. The fact that these ridges have a melt veneer and perched boulders would suggest they were formed during the impact event but before the melt was emplaced or the boulders ejected from the crater, presumably at a late stage in the process. The ridges also exhibit the gentle sinuosity seen in the ridge of Markov E, again suggestive of a common mode of origin (Fig.14). A comparison between Dawes and Sulpicius Gallus serves to illustrate the striking degree of similarity between these two craters, with features to the east of Sulpicius Gallus mirroring 'Rima Dawes'. The oblique nature of the Sulpicius Gallus impact is demonstrated by the Clementine UVVIS Multispectral Mosaic (Fig.15c) indicating an impactor from the north-east, and showing that these ridge like features are again in the uprange direction. These features are not as conspicuous as in Dawes, indeed they are in comparison quite subtle topographically, but the overall morphological similarity and comparable location in relation to the uprange rims are highly suggestive of homologous structures in both craters (Fig.16).

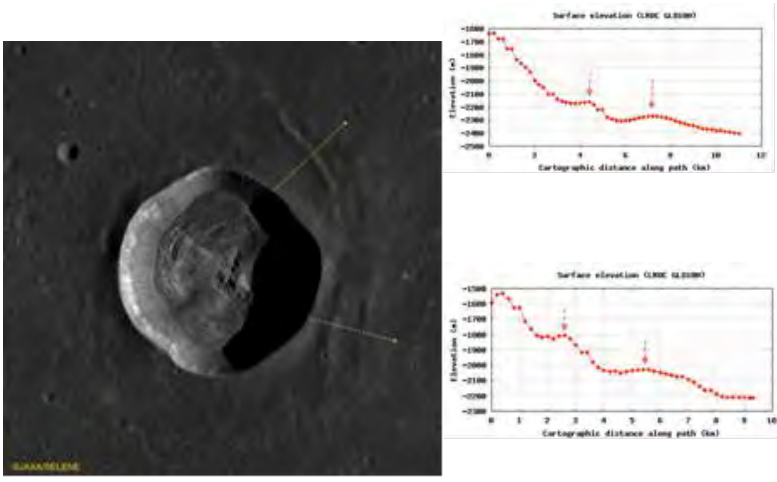

Fig.13 LROC GLD100 surface elevation plots radially from crater rim through 'Rima Dawes'. This shows the inner and outer ridges (red arrows) and the relative topography. Note plots are not equally to scale

The extent of ejecta beyond these uprange ridges in Dawes and Sulpicius Gallus differ in that in the former, conventional ejecta in the form of the 'herringbone' pattern formed by secondary cratering can be traced for approximately 2 crater radii. In the latter case this ejecta is inconspicuous even at one crater radius distance uprange, indicating an overall lack of uprange ejecta development. This would indicate a difference between the two impact regimes, with Sulpicius Gallus representing a shallower impact than Dawes.

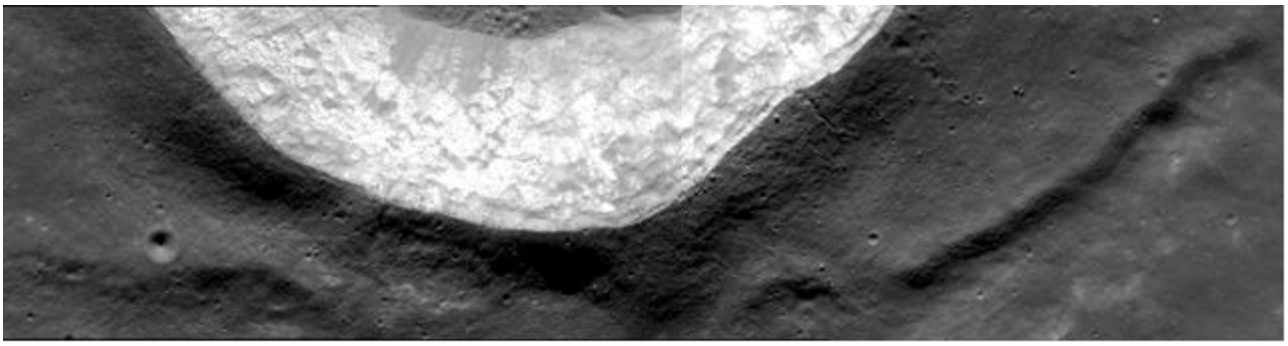

Fig.14 LROC NAC montage of eastern rim of Dawes (north to the right) showing the ridge like nature of the edges of 'Rima Dawes, impact melt gullies in the crater rim and perched boulders on the ridge crests.

a. b. c.

Fig.15 Sulpicius Gallus as viewed by SELENE (a) Apollo 17 (b) and Clementine UVVIS Multispectral Mosaic (c). Note the ridge like structures located to the east of the eastern rim and comparable to 'Rima Dawes'.

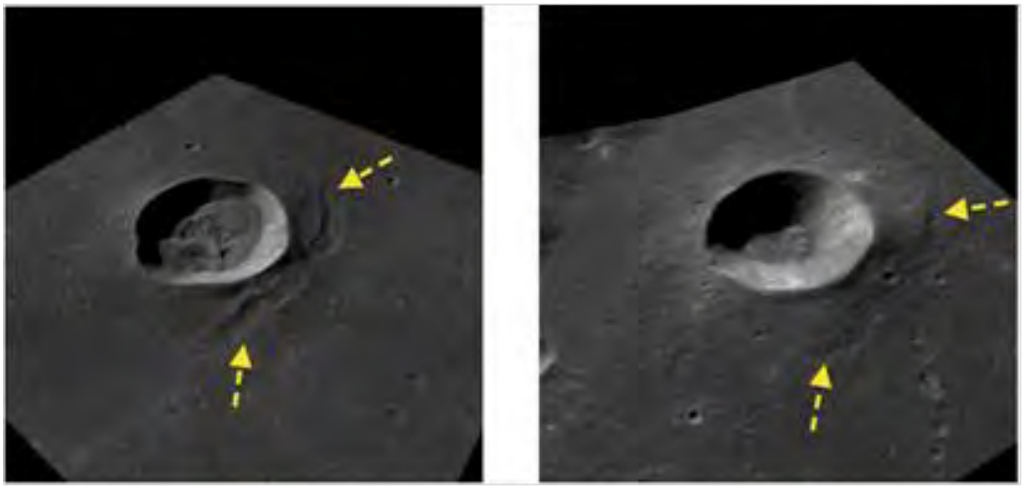

Fig.16 Dawes (left) and Sulpicius Gallus (right) shown from a similar orientation from the uprange direction. Note similar disposition of ridges uprange of both craters as indicated by arrows. (LROC Quickmap 3D Visualisation tool).

Two possible larger examples are seen in Plinius and Picard. Plinius (a close neighbour of Dawes) displays indications of an oblique origin in the form of a depressed rim to the east, but this interpretation may be complicated by a general lowering of the mare surface towards the east at this location. A more convincing indication of oblique impact is provided by the Clementine FeO binned colour image, which shows impact melt of a relatively lower lower FeO content (derived from highland material underlying the mare) preferentially developed towards the west (Fig.17b). If we accept this evidence as indicative of low angle impact origin, an uprange direction to the east is suggested. Immediately to the east of the eastern rim the ejecta blanket can be seen to be developed into a broad ridge that appears to 'wrap' around the northern and southern rims in a crescent shaped structure.

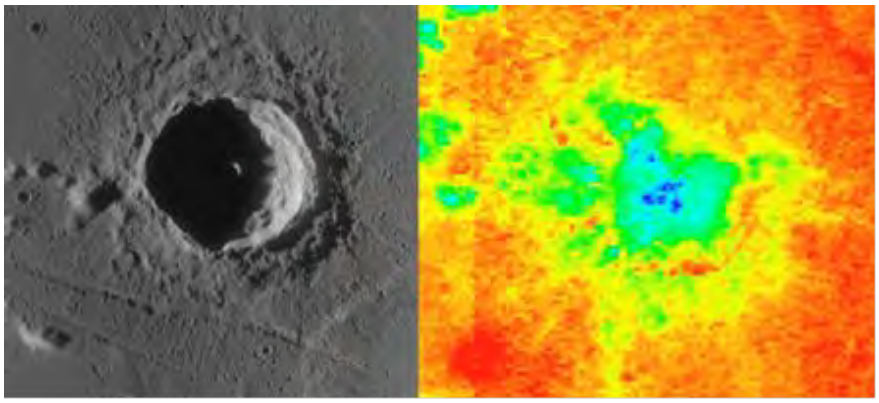

a. b.

Fig.17 LROC WAC montage of Plinius showing uprange ridge (a) and Clementine binned FeO colour map showing downrange bias in ejecta (b).

The ridge can, in places, be seen to be sculpted longitudinally into the now familiar chevron pattern, suggesting an origin in a process similar to that described above (Fig.18). As with Dawes, this broad ridge appears to be developed on the glacis of the crater and grades uprange into a more conventional ejecta blanket with the 'herringbone' texture referred to above to a distance of some 2 crater radii.

Fig.18 SELENE image of Plinius showing chevron patterning in uprange ridge.

The evidence for Picard being an oblique angle impact is subtle, its south eastern rim is slightly depressed in relation to the western, whilst ejecta, in the form of shallow elongate secondary craters, can be traced radially slightly further to the north-west but is still conspicuous to the south-east. This suggests a degree of asymmetry with an uprange direction towards the south-east. As with Plinius, the uprange glacis bears a ridge like rampart, in this example mostly straight, but curving at the ends around the northern and southern crater rims (Fig.19). Indications of the chevron pattern can be seen at either end of the straight section of the ridge, whilst a corrugated texture may indicate a veneer of impact melt.

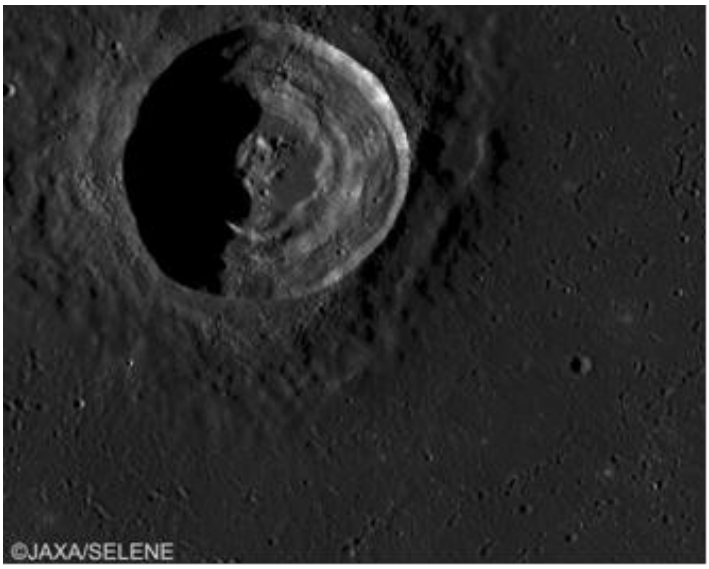

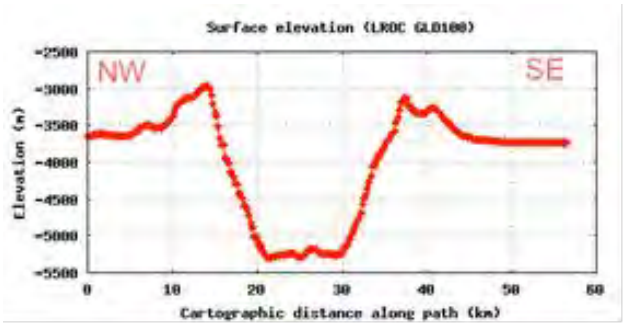

Fig.19 Selene image of Picard showing ridge in uprange ejecta to the south-east (a) and Surface elevation profiles as shown by LROC GLD100 showing depressed rim and ridge on the glacis to the south-east.

This ridge is quite a prominent topographic feature as is shown by the LROC GLD100 surface elevation plot (Fig.19b), whilst its location on the glacis would argue against it being an unrelated pre-impact structure (Fig.20).

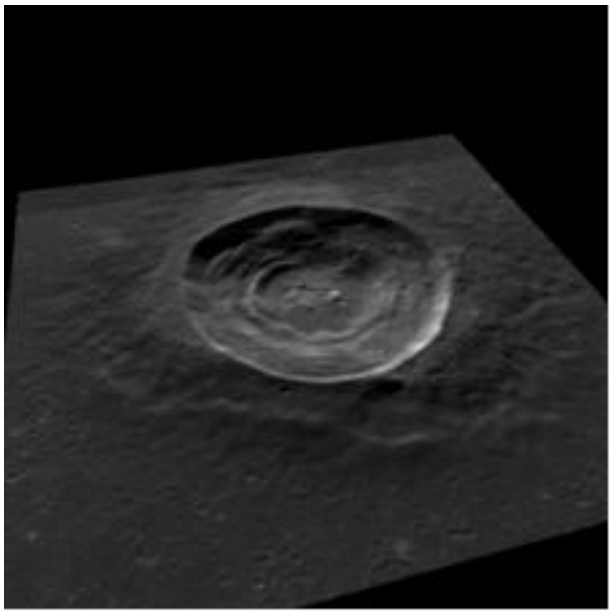

Fig.20 LROC Quickmap 3D Visualisation tool image of Picard as viewed from the east (looking downrange). Note the ridge on the glacis of the south-eastern rampart.

Comparing Plinius and Picard using the LROC WAC Colour Shaded Relief Map (Fig.21) serves to illustrate a final important point. Both craters exhibit indications of enhanced proximal ejecta crossrange, which is a feature of oblique impacts which eventually in the shallowest of impacts (<5º) gives rise to the 'butterfly' pattern of ejecta seen in craters such as Messier (Herrick & Forsberg-Taylor, 2003). This serves to support the interpretation of these craters as being the results of oblique impacts. Neither however show any indication of a ZoA, and as noted both have conventional uprange ejecta in the form of 'herringbone' secondary cratering.

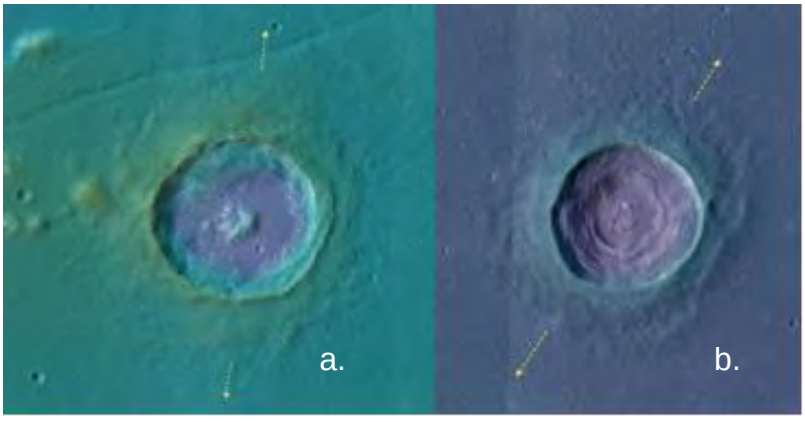

Fig.21 LROC WAC Colour Shaded Relief Map of Plinius (a) and Picard (b) showing enhancement of proximal ejecta crossrange as indicated by arrows. In both cases 'uprange' is to the right.

A final example however provides a possible link between craters with ZoA's and the uprange ridges discussed so far. Harding is an irregularly shaped 22km diameter crater that is not obviously a low angle impact structure. It has however a prominent but extremely wide ZoA, suggesting that the approach angle was well below that required to form a ZoA but clearly above that required to produce a 'butterfly' pattern in the ejecta. The ZoA is not particularly obvious as the southern cardioid ray is far more prominent than the northern one (Fig.22) which appears less conspicuous possibly as a result of compositional differences (possibly with a darker more iron rich lithology contributing to the northern ray).

This gives the crater a somewhat asymmetric appearance, and may contribute to it not being widely recognised as a low angle structure. As with Picard and Plinius a slight crossrange enhancement of ejecta is further indication of an oblique origin. A more detailed examination of the crater rim area reveals a short 'V' shaped trough immediately uprange of the craters north eastern rim, with the apex pointing towards the crater. This feature is extremely subtle (outer ridge ~ 30 to 50 meters high and ~ 2km wide), with little topographic relief and appears to consist of two short (~7km) lunate ridges either side of a shallow trough. Its position mid way between the two cardioid rays of the ZoA, and uprange indicate that it is a feature of the ejecta and not a pre or post impact structure (Fig.23).

In this example it is possible to speculate that this 'V' feature represents an incipient expression of the uprange ridges noted above. What this observation means in terms of the relationship between ZoA formation and ridge formation is a question for further consideration, but it is possible that at different impact angles different features dominate, but this is speculation based on limited observations and the few examples discussed above.

Fig.22 Clementine NIR Multispectral Mosaic of Harding showing the ZoA to the north-east, with brighter southern cardioid ray (a) and Selene montage showing enhanced crossrange ejecta and 'V' structure immediately uprange of the crater rim.

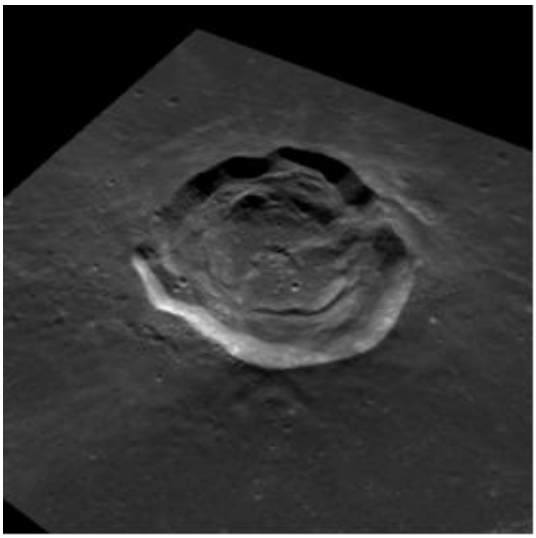

Fig.23 LROC Quickmap 3D Visualisation tool image of Harding viewed from the uprange direction. Note the 'V' feature uprange.

Discussion

The examples described above are intended to demonstrate the existence of an uprange ejecta feature that develops in oblique impacts. At sufficiently low impacts (~15º) a conspicuous ZoA develops where ejecta is sparse uprange. These ZoA's can be bordered by conspicuous bright rays (Proclus, Petavius B), and are also responsible for the diverging uprange ridges ('wings') in older craters, where the bright ray material has been weathered to such an extent that the difference between it and the surrounding surface is no longer obvious (Cauchy, Kies A). The ZoA results from the dynamics of the ejecta curtain, which is initially tilted downrange during the early impact but becomes more upright later in the cratering event. As the impact angle decreases the ZoA becomes wider (as seen in Harding) and eventually gives way to an ejecta distribution which is enhanced crossrange and downrange and absent uprange.

In certain circumstances within these low angle regimes a narrow ridge may form in the uprange ejecta which in some circumstances can result in conspicuous topographic features. It appears that these ridges are produced during the earlier phases of the impact process where the ejection and deposition of ejecta are asymmetric due to the tilting of the ejecta curtain downrange. The ridges may be subject modification, such as impact melt emplacement during later stages of the process when the ejection and deposition of ejecta become symmetric.

The relative infrequency of these ridges may be related to the rather narrow range of conditions during which their formation is possible. It is probable that this process is the result of the complex interplay of a number of factors including impact angle, size and velocity of the impactor, nature and topography of the target and duration of the impact event. The ridges and tangential ejecta features described above may not be directly comparable, the ridge of Markov E and those of Picard and Plinius differ in morphology and scale, but the coincidence of these ridges uprange in oblique impacts suggests the existence of a phase in oblique crater formation that favours enhanced deposition of ejecta material in this location.

References

Elbeshausen,D and Wünnemann, K. 2013 Crater Formation in the Transition from Circular to Elliptical Impact Structures. 44th Lunar and Planetary Science Conference (2013)

Forsberg, N. K., Herrick, R. R., Bussey, B. 1998. The Effects of Impact Angle on the Shape of Lunar Craters. 29th Annual Lunar and Planetary Science Conference, March 16-20, 1998, Houston, TX, abstract no. 1691.

Gault, D. E. & Wedekind, J. A, 1978. Experimental Studies of Oblique Impact, LUNAR AND PLANETARY SCIENCE IX, PP. 374-376.

Herrick, R. R, Forsberg-Taylor N. K. 2003. The shape and appearance of craters formed by oblique impact on the Moon and Venus. Meteoritics & Planetary Science 38, Nr 11, 1551–1578

Schultz, P.H, Anderson, J.B.L and Hermalyn, B (2009) Origin and significance of uprange ray patterns. 40th Lunar and Planetary Science Conference (2009)

Schultz, P.H., J.T. Heineck, and J.L.B. Anderson, 2000 Using 3-D PIV in laboratory impact experiments, in Lunar Planet. Sci. Conf. XXXI, pp. 1902, LPI, Houston, TX

Wood, C, Horns and Wing, LPOD Lunar photo of the Day 18th May 2012 http://lpod.wikispaces.com/May+18%2C+2012

Wood, C, Single Crater Septum, Lunar photo of the Day 19th December 2011 https://lpod.wikispaces.com/December+19,+2011

Acknowledgements

LROC images, topographic charts and 3D visualisations reproduced by courtesy of the LROC Website, School of Earth and Space Exploration,University of Arizona at: http://lroc.sese.asu.edu/index.html

Clementine Multispectral Images courtesy of the USGS PSD Imaging Node at: http://www.mapaplanet.org/

Apollo images courtesy Lunar and Planetary Institute web site at: http://www.lpi.usra.edu

Selene images courtesy of Japan Aerospace Exploration Agency (JAXA) at: http://l2db.selene.darts.isas.jaxa.jp

LEAVING NO DOME UNTURNED

Review reprint from LPOD by C. Wood

Over the last ten years or so a small international group of professionals in various fields relentlessly imaged, measured and analysed lunar domes. They started with their own images and traditional techniques, and embraced new data and tools as they became available from orbiting spacecraft to refine their calculations and increase the types of knowledge gained. Early on simply getting an accurate determination of dome height and slope was a significant advance, and now they routinely estimate surface compositions, eruption conditions and geophysical constraints of dome formation. It is not an exaggeration to say that with the publication of the first book devoted exclusively to domes that Raf, Christian, Jim and Maria Teresa have become the world's leading experts on these small volcanoes. The first third of the book is technical, reflecting its origin in papers the team has published in professional journals, The rest is a mare by mare observer's guide to many dozens of domes, each illustrated with spacecraft and amateur images, and derived topographic profiles. The book is not for the casual observer, but both the professional lunar geologist and the advanced amateur will want it as a compact handbook of virtually everything we know of some of the Moon's most illusive features. These same four people are the leaders of the Geological Lunar Researches Group that has recently published the 31st issue of Selenology Today, a high level journal that provides opportunities for amateurs to publish new research on the Moon. Congratulations to GLR for ST and Lunar Domes.

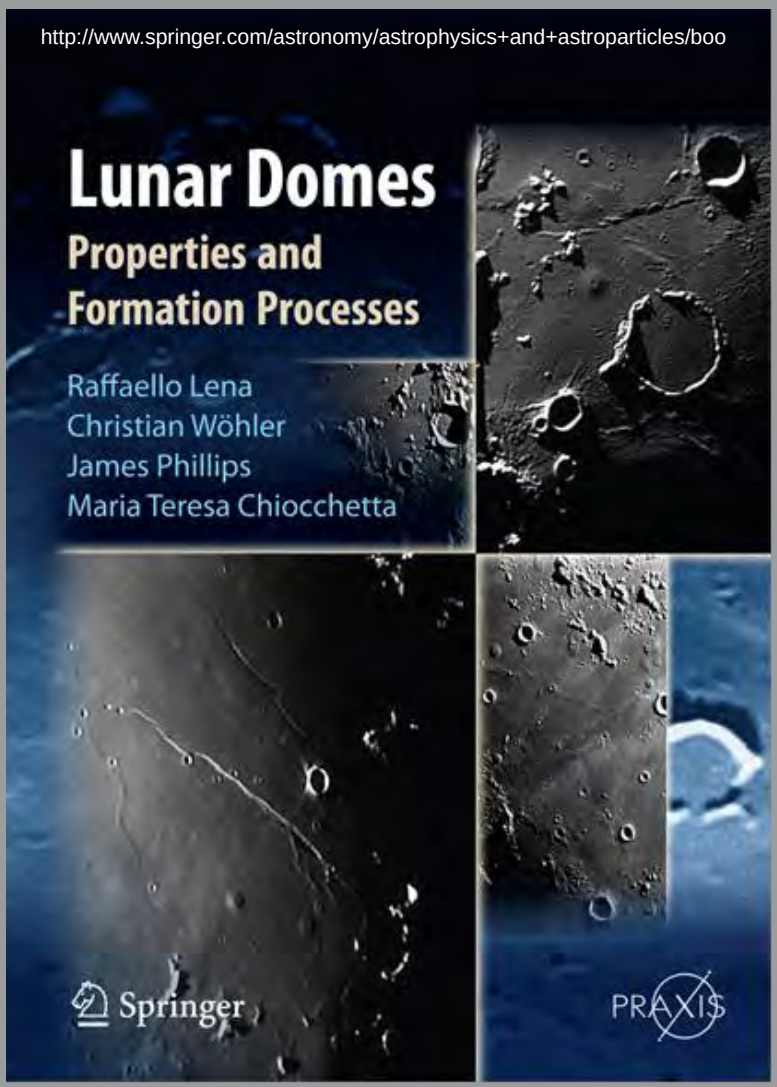

Image from Springer

Chapter 1

This chapter provides an overview of terrestrial and lunar volcanic processes. The dependence of the shape of a volcanic construct on the physical and chemical properties of the erupting lava is described. Furthermore, an introduction to lunar pyroclastic deposits, lunar cones and effusive lunar domes and their vents as well as an outline of the occurrence of different types of volcanic constructs on the Moon and the corresponding formation mechanisms is given.

Chapter 2

This chapter describes different methods for determining the morphometric properties (diameter, height, flank slope, volume) of lunar domes, a model to estimate the physical properties of the dome-forming magma, and different classification schemes for lunar domes.

Selenology Today

Chapter 3
This chapter gives an outline of methods for describing the lunar surface in terms of specific spectral parameters inferred from multispectral or hyperspectral image data. These allow for the detection of specific lunar minerals, an estimation of the abundances of important chemical elements, and a mapping of the lunar surface in terms of its basic petrographic constituents.

Chapter 4
This chapter describes how the dimensions of the dikes through which the dome-forming magma ascended to the surface can be modelled. Furthermore, a modelling approach to encompass the physical conditions under which putative intrusive lunar domes were formed is outlined.

Chapter 5
This chapter describes a classification scheme for lunar domes which relies on the spectral and morphometric parameters by which they are characterised, the rheologic parameters describing the dome-forming magma, and the physical conditions under which dome formation occurred.

Chapter 6
This chapter provides an overview of effusive lunar domes bisected by linear rilles. A description of the formation conditions is provided according to the modelling approaches described in the previous chapters.

Chapter 7
This chapter provides a detailed description of a large number of lunar domes in a variety of regions according to their determined spectral and morphometric properties as well as the inferred rheologic properties of the dome-forming magma and the corresponding feeder dike dimensions.

Chapter 8
This chapter provides a discussion of the putative lunar intrusive domes, their morphometric properties and the conjunction of the large specimens with linear rilles.

Chapter 9
This chapter provides a summary of the book and gives a perspective towards future research activities regarding lunar domes.

Lunar dome Properties and Formation Processes
Series: Springer Praxis Books
Subseries: Astronomy and Planetary Sciences
Lena, R., Wöhler, C., Phillips, J., Chiocchetta, M.T.

2013, XIII, 174 p. 145 illus., 10 illus. in color.

http://www.springer.com/astronomy/astrophysics+and+astroparticles/book/978-88-470-2636-0

Selenology Today

On the imaged short and narrow rille near Rima Sheepshanks

By KC Pau and R. Lena
Geologic Lunar Research (GLR) group

Abstract
During a survey we detected a small fine rille to the south of the main Rima Sheepshanks. The unnamed rille, likely an extension of the rille segment from Rima Gartner, was initially detected in 2003 with a Toucam camera. We report our imagery displaying the narrow rille, which is shown in the LROC WAC imagery and Clementine imagery.

There are so many rilles existing on the surface of the Moon. Some of them are very easy to locate, such as the most renowned Triesnecker complex rilles system and the Hippalus rilles system. There are some rilles that need an appropriate illumination condition to identify them, such as the Rima Sheepshanks. In this study we examine a small rille located to the south of the Rima Sheepshanks.
Possibly it is a rille segment connecting Rima Sheepshanks and Rima Gartner. A description of the complex rille system, examined in this report, is reported by Wood in a previous LPOD

(http://lpod.wikispaces.com/May+14%2C+2010)

According to Wood (2010) the complex system of rilles were poorly known and in our knowledge also imaged.
The narrow rille or rille segment was detected by KC Pau and also imaged by Lena using telescopic CCD images. It is not reported in the Atlas of the Moon by A. Rükl, in the Lunar Quadrant Maps and in the LAC charts.
Initially, Pau imaged it on December 29, 2003 with a Toucam camera and a 250 mm Newtonian telescope (Fig. 1). It is marked by arrows and lies to the south of the main Rima Sheepshanks.
On April 27, 2012, Lena took some AVI clips of the Sheepshanks region using a 180 mm Mak-Cassegrain Telescope. The subtle rille or rille segment was easily detected and the image, made at 19:21 UT, is shown in Fig. 2 (top and bottom for high enlargement).

Another recent image was taken by Pau on February 17, 2013 at 11:56 UT with a 250 mm Newtonian telescope (Fig. 3). Moreover the image displays both the whole length of Rima Sheepshanks and the examined feature. However the rille is well detectable in the Lunar Reconnaissance Orbiter (LRO) WAC imagery, which displays this elusive rilles system (cf. Fig. 4) and in the Clementine imagery (Fig. 5).
The narrow rille, located between Gartner C and Galle F, is running to the east-northeast, exactly like Rima Sheepshanks and can be a target for further imagery.
It is apparently a linear graben, like the Rima Sheepshanks. Lunar linear graben probably are the surface expressions of intruded dikes that fill extensional weak zones radial to basins. However no albedo variations are detectable in this region and near the rille suggesting the absence of pyroclastic material, as it is the case for the magmatic origin for Rima Hyginus. The size of telescope is definitely an important factor in detection of fine rilles or domes. The seeing is the most important factor. If the seeing is steady, the resolution of the image taken with our telescopes can be comparable with larger size telescopes. The detection of "subtle" or “news” features on moon needs patience. Most amateurs nowadays only doing casual imaging and observation of the moon. Our aim of imaging is to find something and keep records of most features in different illumination. That's the first target and principle of the GLR group.

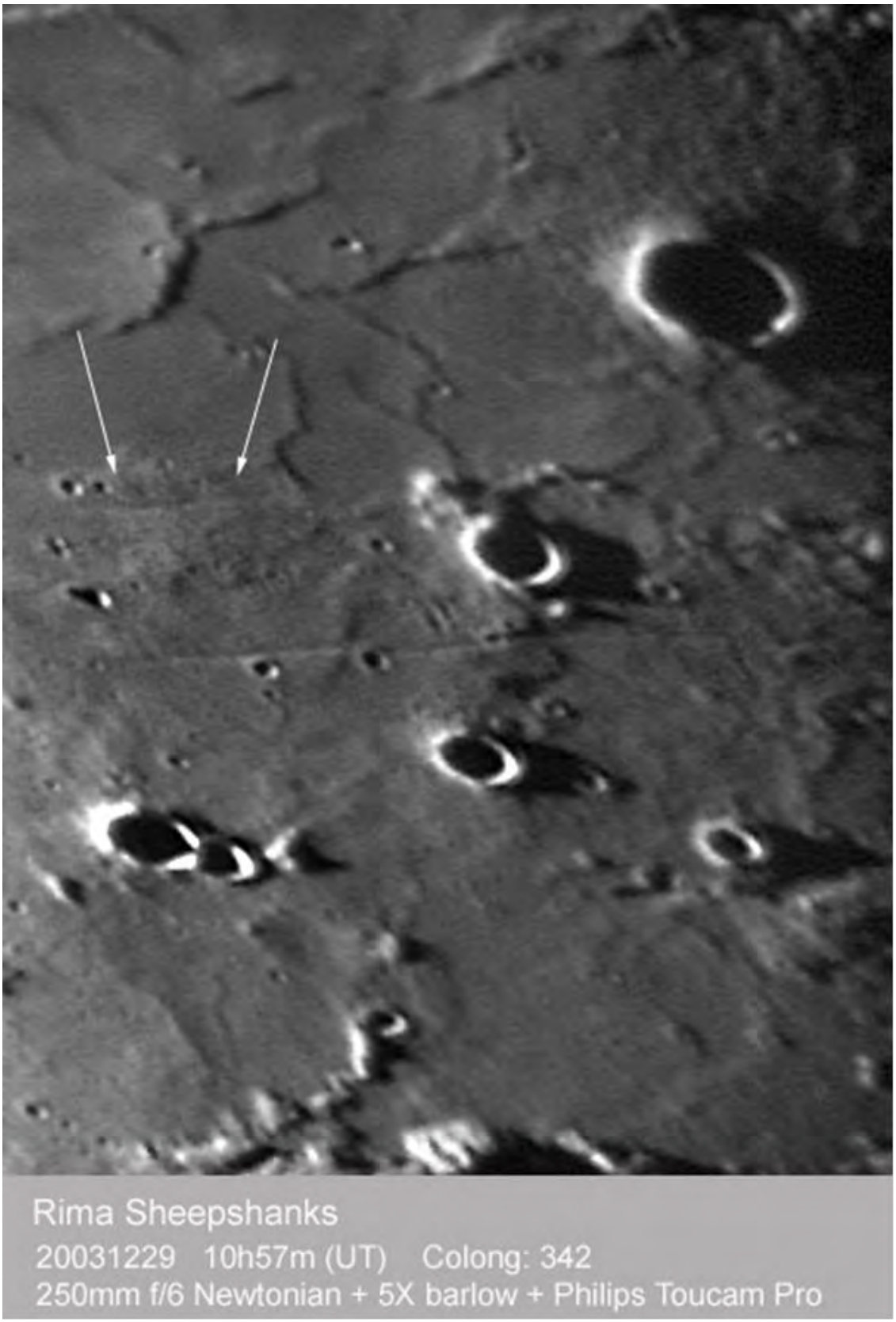
Rima Sheepshanks
20031229 10h57m (UT) Colong: 342
250mm f/6 Newtonian + 5X barlow + Philips Toucam Pro

Fig. 1

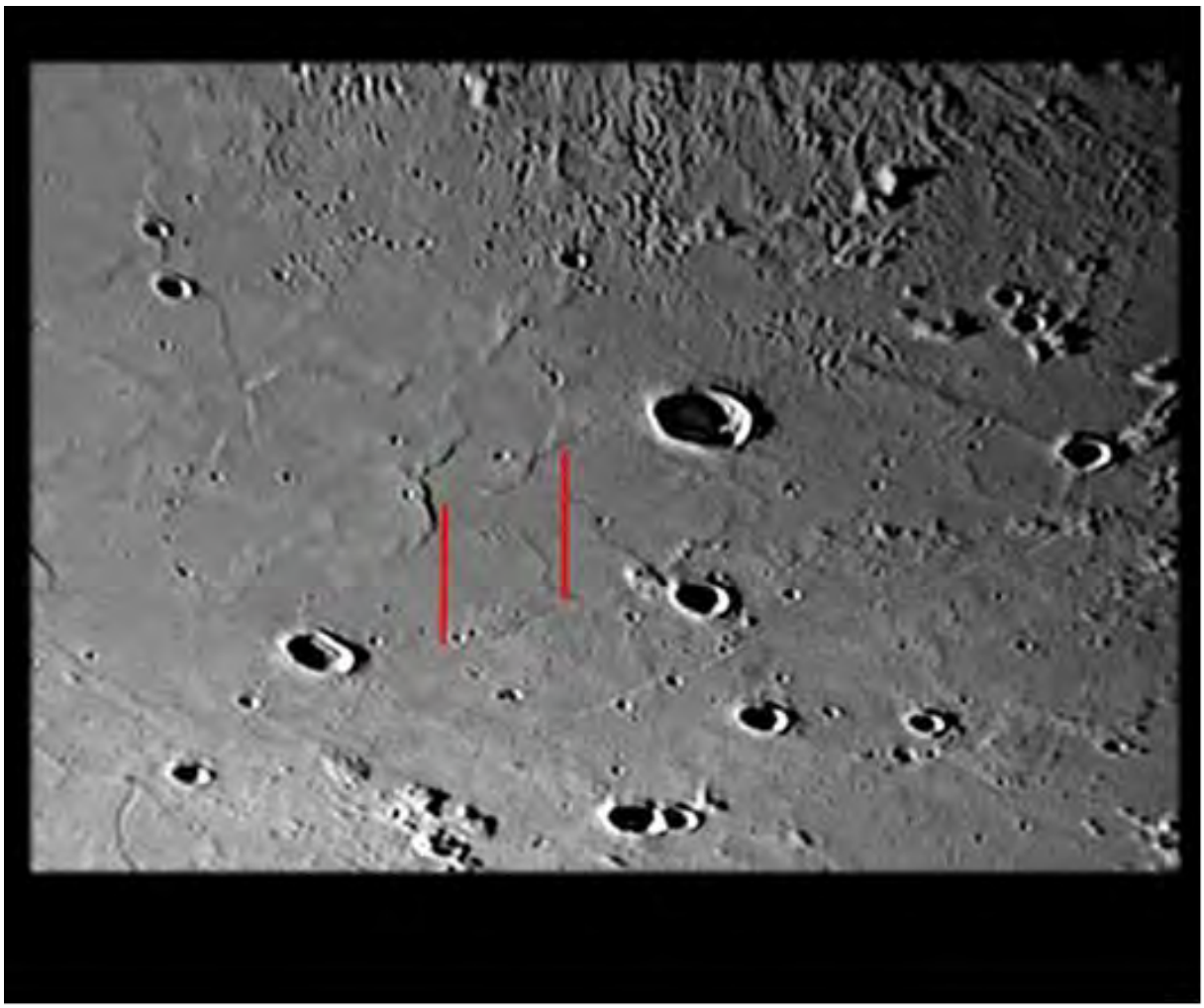

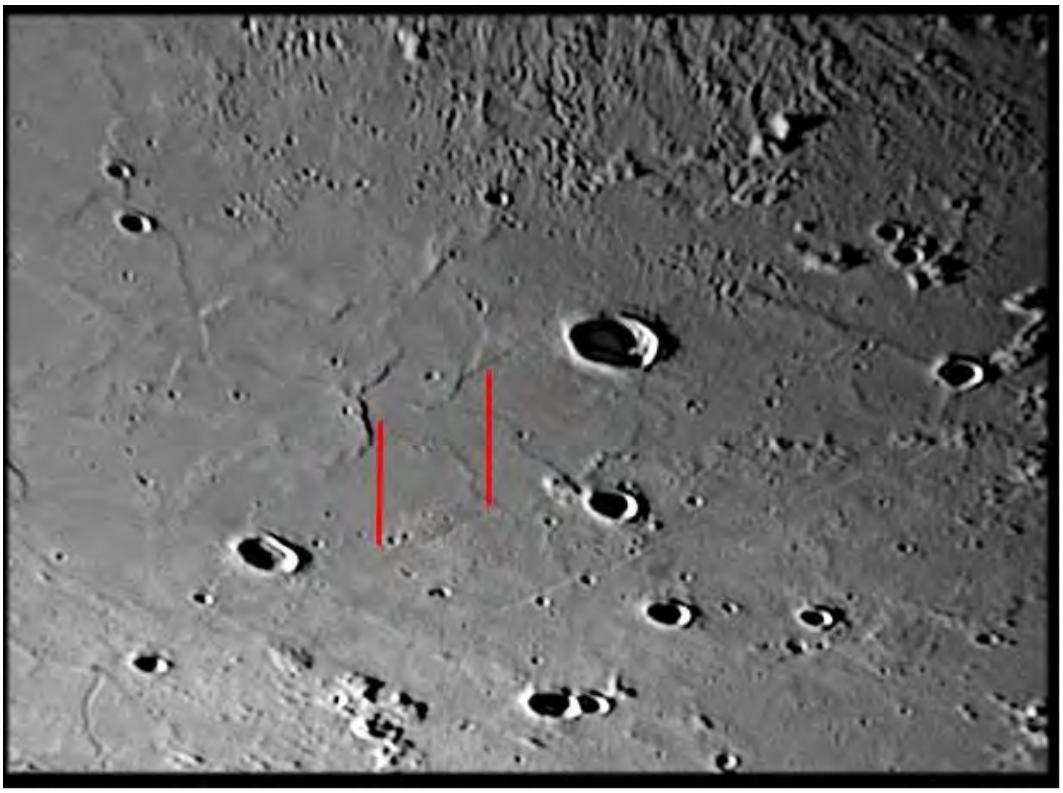

Fig. 2

Rima Sheepshanks

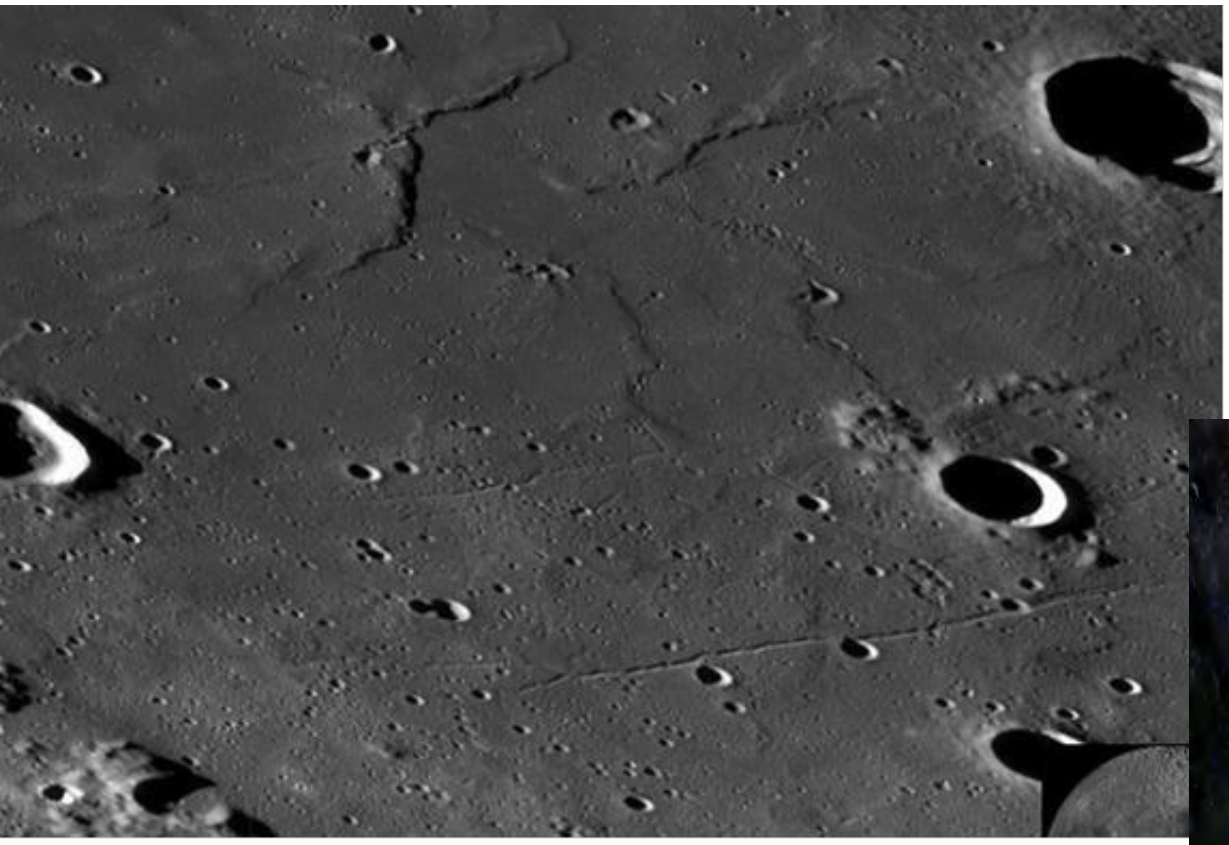

Fig. 4

Fig.5

Selenology Today

Unusual Crater Ejecta Feature.

Barry Fitz-Gerald GLR Group

Abstract

Impact crater ejecta takes a wide variety of forms including rays and secondary craters which are produced by the excavation of target material and their expulsion from the transient cavity during crater formation. The material excavated in most cases ends up distributed more or less symmetrically around the crater, with only very low angle impacts producing asymmetric distributions. Infrequently an ejecta field will strongly reflect the azimuthal direction of the impactor, with features such as a Zone of Avoidance or Forbidden Zone in the uprange direction (such as Proclus) or conspicuous downrange rays (such as Messier A) forming. The current article describes an unusual uprange feature which takes the form of a linear gouge extending away from a small (~1.2km) very oblique angle crater on the south eastern rim of Vasco da Gamma B.

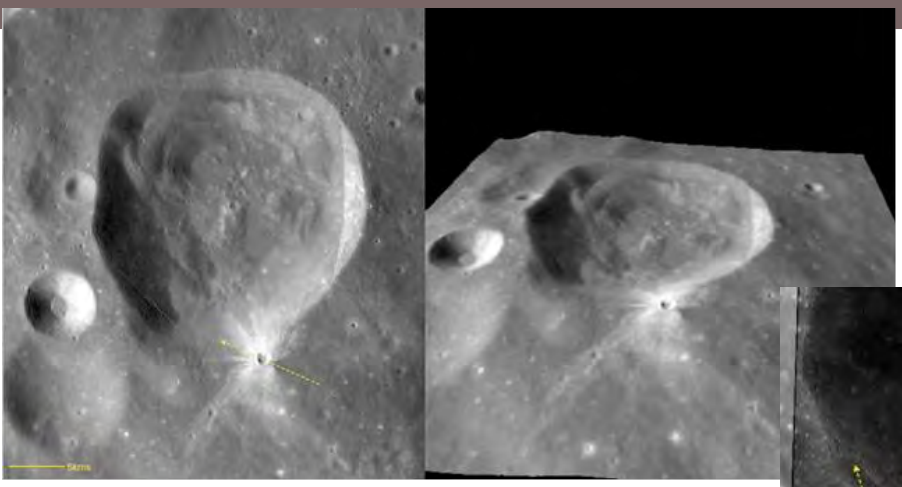

Fig.1 LROC image of oblique angle impact (crater X) on the south eastern rim of Vasco da Gamma B, dashed arrow shows approximate trajectory (a), and LROC Quickmap 3D Visualisation tool image showing terrain at impact site (b).

The crater discussed appears to be the result of an exceedingly shallow angle impact of a small body travelling from the south east, with the rim of Vasco da Gamma B (for brevity referred to as VdG.B in the following text). The impact appears to have struck the very crest of the rim of VdG.B, and occurred as a such a shallow angle that the resulting crater (referred to as crater X) was not excavated to any great depth, and probably no more than a few tens of meters.

As can be seen in Fig.1 VdG.B itself has a somewhat 'teardrop' shaped outline, and abuts a raised massif like area to the south east. The oblique nature of crater X is indicated by the conspicuous dark Zone of Avoidance (ZoA) to the south-east and the 'butterfly' pattern ejecta laterally, with the southern 'wing' developed downslope and the northern one along the eastern rim of VdG.B.

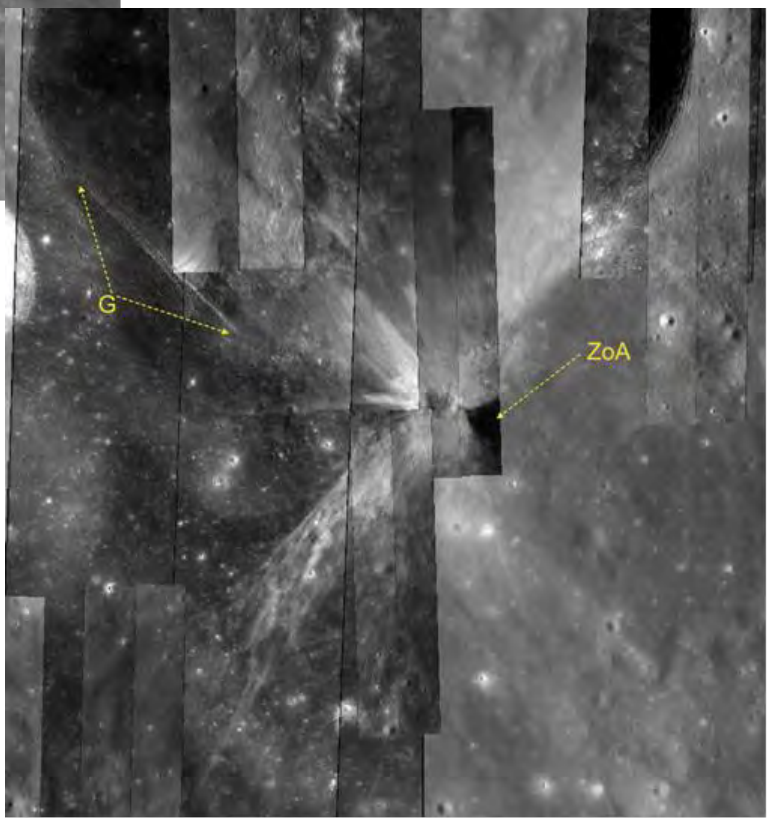

Fig.2 LROC image showing crater X with prominent dark Zone of Avoidance (ZoA) and gouge like furrow (G) along the inner south-western wall of Vasco da Gamma B.

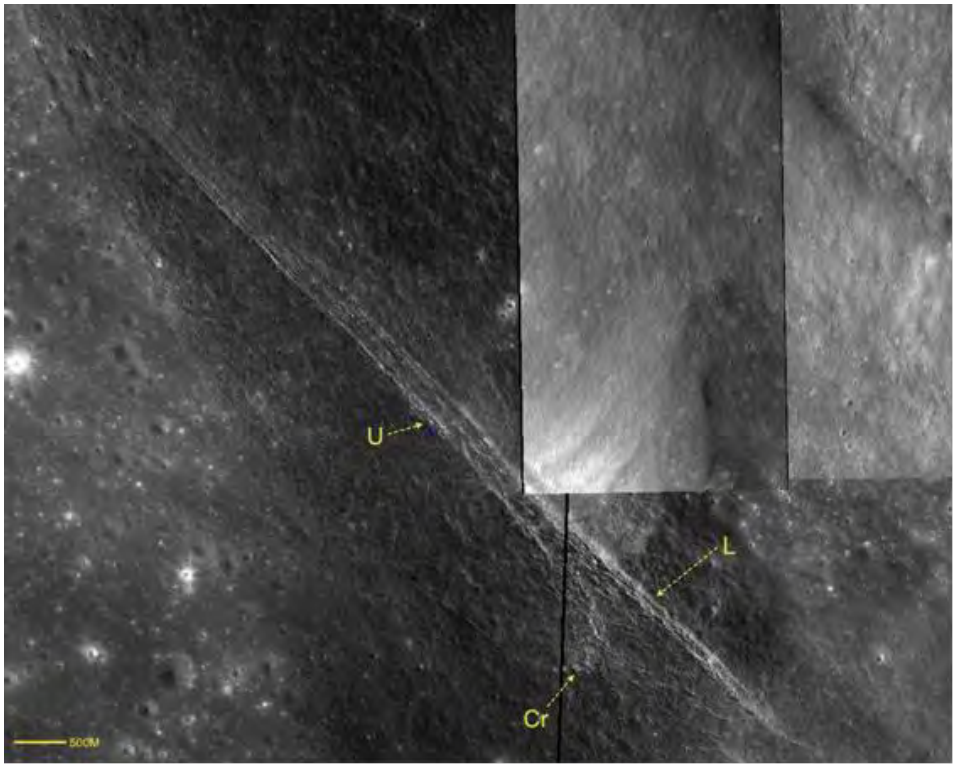

Fig.3 LROC image of gouge like feature showing upper (U) and lower (L) grooves and crescent shaped scar (Cr) that appears to grade into the upper groove distally.

A more detailed view of crater X as shown in Fig.2 reveals that in the downrange direction the inner wall of VdG.B bears a gouge like linear feature that extends for some 9kms towards the north-west and measures approximately 300 meters wide. In close up this gouge appears to form, for much of its length, a pair of ragged grooves cut into the inner crater wall of VdG.B, appearing more prominent proximally, and less so distally (in this context 'proximal' means proximal to crater X). For the proximal 1/4 of its length the gouge consists only of the lower groove whilst up-slope of this is a crescentic scar which is convex proximally and concave distally. The lower 'horn' of this crescent appears to grade distally into the upper of the two grooves that form the remainder of the gouge like feature (Fig.3).

Each groove appears to be cut into the inner crater wall of VdG.B and to have exposed fresh immature regolith that has formed numerous small avalanches and debris slides which in places have cascaded down towards the crater floor of VdG.B. One particularly prominent area of slumping is marked by high albedo fans of debris which are criss-crossed by numerous discontinuous boulder trails indicating that the rocks forming them travelled downslope at some considerable velocity and in a saltatory type of motion. Numerous other small debris slides mantle the grooves themselves, some coming to rest in lobate fronts on the shelf like lower surface of the grooves.

These smaller debris slides appear to have a low albedo and may represent slumps of mature regolith from inner crater wall surface higher up-slope (Fig.4). The USGS Map-a Planet Ratio Map images give an indication of the amount of disruption caused to the inner walls of VdG.B as can be seen in Fig.5. Here the disrupted crater wall of VdG.B is conspicuous due to the bright blue colouration of the exposed immature material in the gouge and on the slopes above and below.

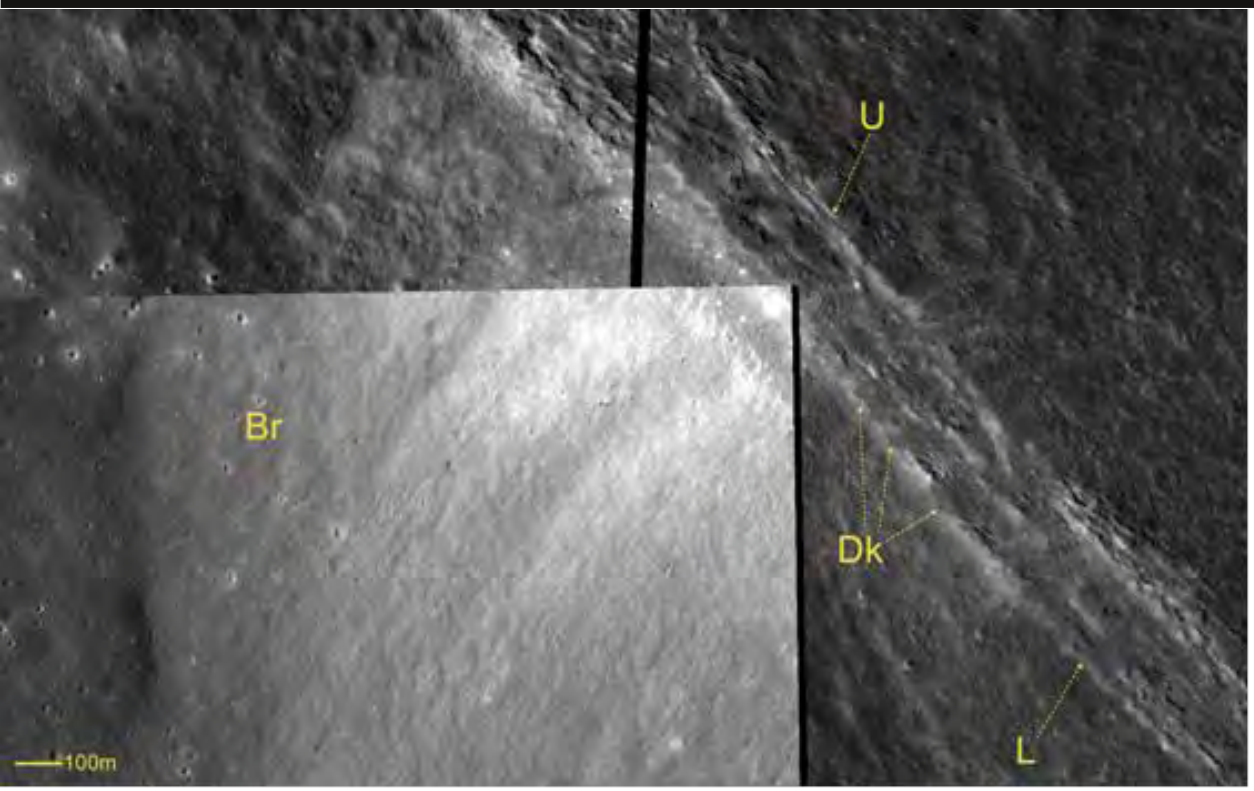

Fig.4 LROC image showing upper (U) and lower (L) grooves, dark debris slides (Dk) and high albedo debris fans crossed by boulder trails (Br). (Note 'proximal' is towards upper left)

Fig.5 Clementine UV-VIS Ration Map image of crater X showing bright immature ejecta including butterfly wings. The gouge like feature and disruption to the inner crater wall of Vasco da Gamma B are also picked out in bright blue (showing the presence of immature regolith).

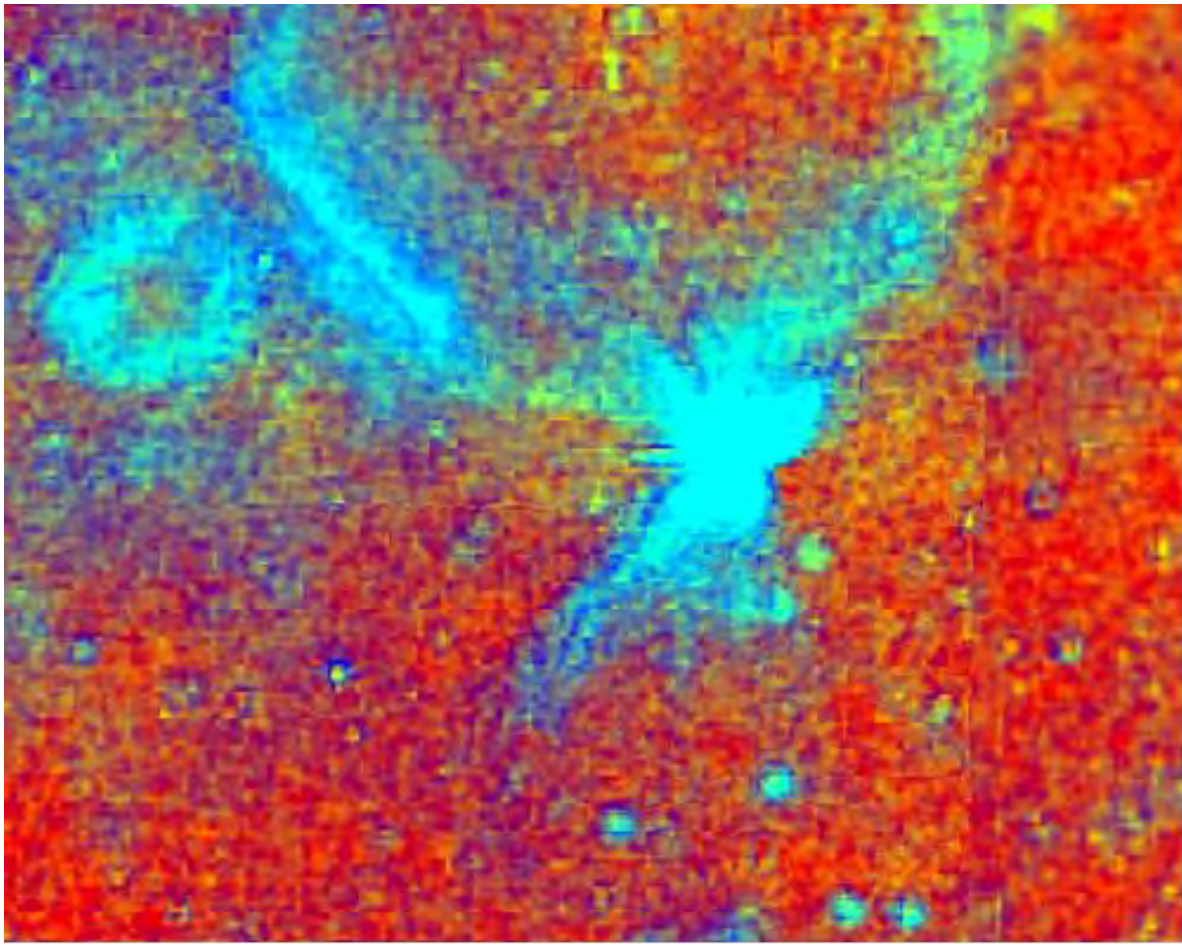

Crater X itself is 'D' shaped in planform, with the straight side of the 'D' forming the up-range rim and the convex side the downrange (Fig.6). The crater floor is littered with both light and dark boulders (possibly indicative if a variable lithology) as well as in-situ exposures of country rock from which the boulders are derived, but there are no conspicuous areas of impact melt. In the ejecta field immediately downrange (to the north west) at least two narrow sinuous features ending in lobate fronts may indicate impact melt channels, these may however be interpreted as debris slides of unconsolidated fine ejecta and not melt. In this downrange field a number of fine boulder trails can be seen descending over 1km in height and 2km in distance from crater X towards the floor of VdG.B. Crater X lacks a raised rim, possibly as a consequence of the very low angle of impact.

There is a vertical height difference of some 1.2kms between the downrange edge of crater X and the start of the gouge feature which is some 8kms further downrange to the north-west. It is also apparent that a line drawn from the proximal end of the gouge south-eastwards through crater X bisects the ZoA and therefore lies in line with the inferred trajectory of the original impactor. This would suggest that if this gouge was caused by ejected material from crater X, that this material travelled from the impact site on a downwards trajectory of some 9° (Fig.7).
In contrast to this, the gouge feature itself is inclined upwards at an angle of approximately 6.5° from its proximal end towards its termination near the south-western rim of VdG.B. The direction of the gouge however is not a continuation of this line, but deviates to the north by approximately 30°,

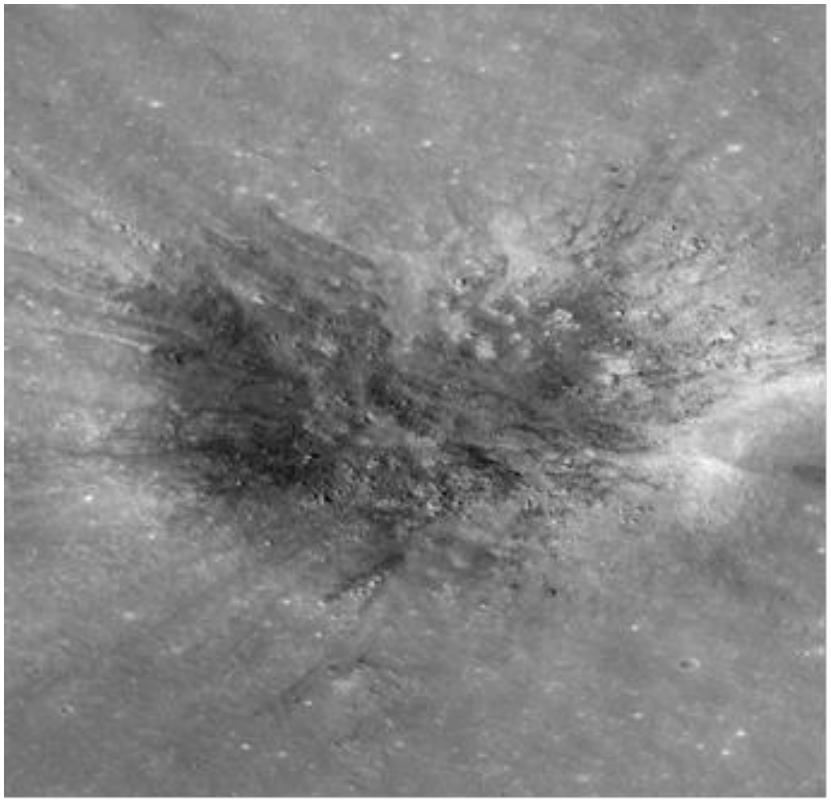

Fig.6 LROC image of crater X showing blocky nature of floor with mass of light and dark boulders possibly indicating a heterogenous lithology at this location. Impactor approached from lower right.

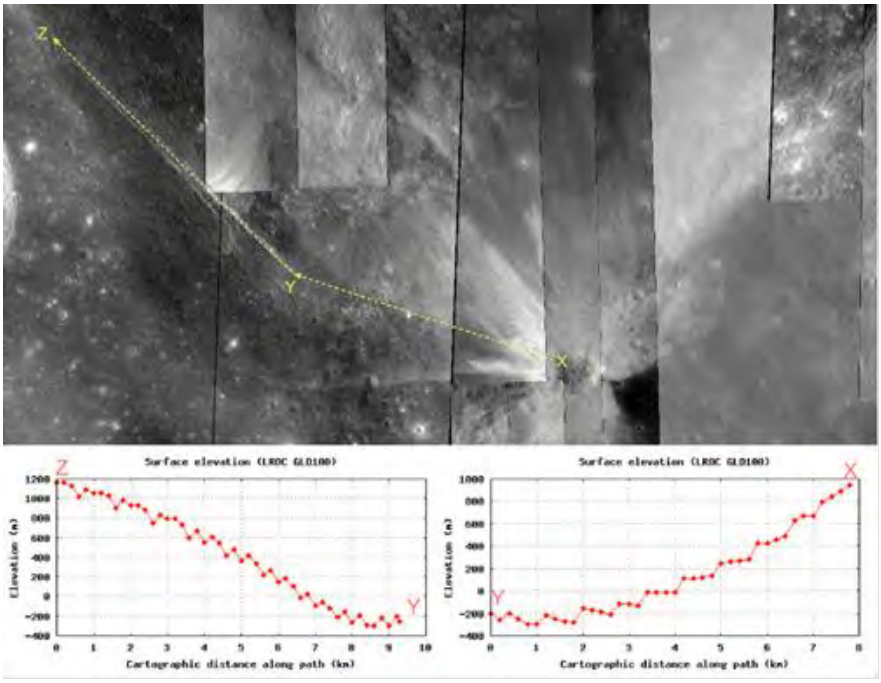

Fig.7 Surface elevation profiles showing downwards trajectory from crater x to proximal end gouge (X-Y) and upwards trajectory of groove forming objects (Y-Z). Note deflection of trajectory at Y.

indicating that the impacting objects were deflected by the impact with the inner crater wall of VdG.B both in azimuth and altitude. It must be stressed however that this is just a qualitative view and no precise geometric analysis has been conducted to support this proposition. The inner crater wall of VdG.B between crater X and the proximal end of the gouge did not escape the ravages of ballistic erosion, and linear striations orientated in an approximate east to west direction can be seen incised into its surface, below which are rocky exposures that appear to have produced a small cascade of boulders which have left trails on the slope towards the crater floor (Fig.8). It is possible that these features were produced as a consequence of the impact that produced crater X and the propagation of high velocity debris downrange.

At the very distal end of the gouge below the south western rim of VdG.B a small pit may represent a small crater produced by the final surviving fragment of the object(s) producing the grooves, above the pit the rim of VdG.B appears to have undergone a slight episode of slumping.

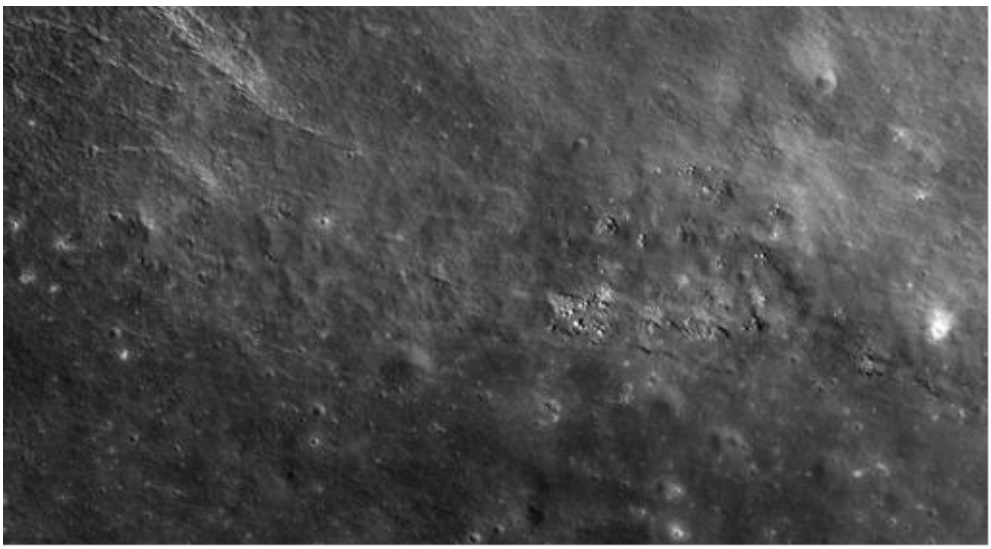

Fig.8 LROC view of southern inner crater wall of Vasco da Gamma B showing dark striated surface (lower edge of frame) and rocky exposures possibly produced by impact of ejecta from crater x. Note the proximal end of the gouge visible top left.

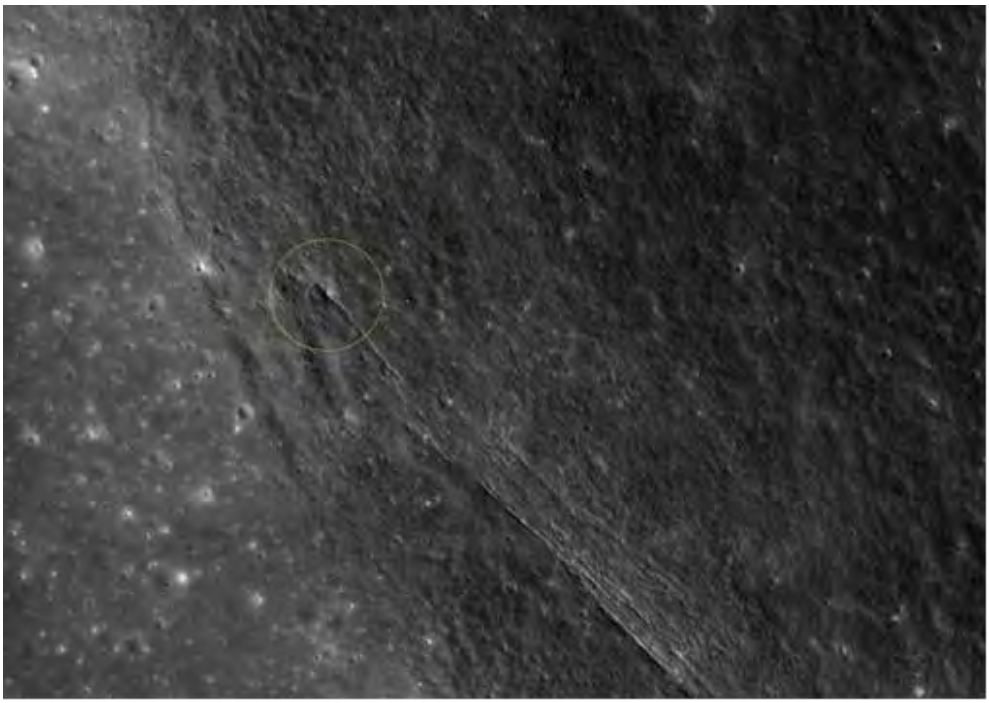

Fig.9 Small pit or crater (circled) at the distal end of the gouge feature just below the south-western rim of Vasco da Gamma B.

Discussion

It would be fair to say that the most likely origin for the gouge like feature seen in the above example, is as a result of high velocity debris travelling on a grazing trajectory along the inner crater wall of VdG.B from an origin in crater X. The morphology of the gouge would suggest that this material took the form of at least two discrete objects (or groups of tightly associate objects) which formed the upper and lower grooves, and a train of objects of variable size drawn out in a vertical line giving rise to the crescentic scar. The objects that formed the upper and lower grooves would appear to have impacted and then travelled some 9kms or so, ploughing grooves into the inner crater wall of VdG.B. It is probable that as these objects travelled downrange they were disrupted into smaller fragments which would account for the shallowing and narrowing of the grooves to the north-west.

As noted above, the orientation of the gouge feature is deflected northwards by some 30° relative to the proposed impactors azimuth, and is elevated in altitude by some 6.5 relative to its initial origin. The remarkably straight course of the gouge downrange thereafter suggests that the groove forming object or objects possessed considerable kinetic energy, possibly greater than that normally partitioned into conventional cater ejecta. This observation raises the possibility that the groove forming objects were not crater ejecta (material excavated from crater x and expelled during the crater forming process) but a fragment or fragments of the original impactor travelling along their original trajectory, and with a high proportion of their pre-impact velocity. This may be a consequence of impactor decapitation where the impactor experiences shear failure during the crater X event producing daughter fragments which continue along the original trajectory to impact further downrange.. Such processes are thought responsible for many impact structures (Schultz & Gault 1990) with Messier and Messier A being prime examples, whilst impactor decapitation has also been implicated in the production of basin size structures (Stickle et.al, 2012). In the present case sufficient energy was released in the crater X impact event to produce an extensive ejecta blanket consistent with an oblique angle impact, as well as excavating a crater, albeit a very shallow one, but part of the impactor escaped destruction at this point and continued onwards to create the gouges and striations we see downrange.

If this gouge is a result of impactor decapitation, it might suggest that similar structures exist elsewhere but have not been identified as impact related structures. The present example is particularly conspicuous due to the relative youth of crater X and the presence of bright immature ejecta, which if absent would make the identification of similar structures difficult.

References

Schultz, P. H. & Gault, D. E. 1990 DECAPITATED IMPACTORS IN THE LABORATORY AND ON THE PLANETS; Abstracts of the Lunar and Planetary Science Conference, volume 21, page 1099

Stickle, A.M., Schultz, P.H and Crawford, D.A, 2012. EFFECT OF ASTEROID DECAPITATION ON CRATERS AND BASINS. 43rd Lunar and Planetary Science Conference

Acknowledgements

LROC images and topographic charts reproduced by courtesy of the LROC Website at http://lroc.sese.asu.edu/index.html, School of Earth and Space Exploration, University of Arizona.

Clementine UVVIS Clementine UV-VIS Ration Map image courtesy of the USGS PSD Imaging Node at http://www.mapaplanet.org/

Torricelli

By Richard Hill Loudon Observatory

Torricelli along with the rest of Sinus Asperitatis was imaged on May 16, 2013 at 02:19 UT (Fig. 1). This is a region of irregular craters from Hypatia on the left edge to Isidorus B in the right half of the image. I would call your attention to Censorinus C just above Isidorus B. Look at the floor of this crater. On LROC Quick Map it appears to be filled with ejecta from one of the local impacts (Theophilus?). It is a very complex structure. The finest craters identified in this image were about 1.5 km across. The images were stacks of 300 frame from 1500 frame AVIs using Registax6. The 3 images were then further processed with GIMP and IrfanView and finally assembled with AutoStitch. Torricelli has been a favourite of mine for decades since first observing it with my old 2.4" refractor in the early 1960s. After Triesnecker it may be the most imaged feature I've done on the Moon.